공학박사 학위논문

Degradation of surface film on $LiCoO_2$ electrode at moderately elevated temperature and its effect on cell properties, and the countermeasures

$LiCoO_2$ 전극 표면필름의 고온 퇴화와 이의 전지특성 영향 및 그 완화방안

2018 년 8 월

서울대학교 대학원

화학생물공학부

정 혜 정

Abstract

Degradation of surface film on $LiCoO_2$ electrode at moderately elevated temperature and its effect on cell properties, and the countermeasures

Hyejeong Jeong

School of Chemical and Biological Engineering

Seoul National University

Lithium-ion batteries (LIBs) are one of the most popular energy conversion and storage devices, currently, used in electronic devices and electric vehicles. Because they can be heavy-duty used or abused, LIBs are frequently exposed to moderately elevated temperature (ca. 60-100 ° C). LIBs are often degraded at the temperature. The cell' s life is shortened or safety problems are caused. Therefore, to unravel the failure mechanisms of LIBs at moderately elevated temperature, and to find the appropriate countermeasures are very important.

Surface films on electrodes generated by reduction/oxidation of electrolytes are electrically insulating, so further electrochemical decompositions of electrolyte are prevented. It is the passivating role of the surface films. It is known that surface films on the negative electrode are damaged, and lose its passivation ability. Electrolyte is electrochemically decomposed on the damaged and naked electrode surface, leaving new films on the electrode. This process leads to capacity fading and shortened cell life. Compared to surface films of negative electrodes, these studies are insufficient for surface films of positive electrodes.

Based on the discussion above, the objectives of this study are to reveal the degradation of surface film on $LiCoO_2$ electrode at moderately elevated temperature and its effect on cell properties, as one of the failure mechanism of $LiCoO_2$ electrode, and to suggest an appropriate countermeasure. (1) In the first part, it is attempted to reveal whether the surface film on the $LiCoO_2$ positive electrode is degraded upon exposure to moderately elevated temperature, if yes, what is the cause, and how the film degradation affects the cell performances. (2) In the second part, when the cell is exposed to elevated temperature at higher State-Of-Charge (SOC), how surface films behave, and how it affects cell performances are studied. (3) Finally, it is tried to suppress degradation of surface film at moderately elevated temperature to mitigate degradation of the cell.

To reduce HF in the cell, which is the cause of surface film degradation at the temperature, CuO is added into $LiCoO_2$ electrode as a HF scavenger.

To simulate the high-temperature exposure, Li/$LiCoO_2$ cells were fabricated and cycled to deposit surface films on the $LiCoO_2$ surface, and then stored at moderately elevated temperatures (60 or 70 ° C). To investigate surface film degradation, the cells were stored at fully discharged state. To investigate the effect of SOC of the cell, they were stored at somewhat charged state. After the storage, the cells were cycled again at 25 ° C to check for signs of cell degradation. CuO-added $LiCoO_2$ electrode and Li/$LiCoO_2$ (CuO-added) cells were fabricated and stored at same conditions with above. Postmortem analyses were performed on the damaged $LiCoO_2$ electrodes.

As a result, (1) in the first part, it was revealed that the surface films on the $LiCoO_2$ positive electrode is degraded at 70 °C, and it is caused by HF attack from $LiPF_6$ salt. After storage, electrolyte oxidation occurs on damaged $LiCoO_2$ surface and charge capacity of Li/$LiCoO_2$ cell increases and Coulombic efficiency decreases. (2) In the second part, it was revealed that when the cell is exposed to elevated temperature at higher SOC, surface films are repaired due to electrolyte oxidation on the degraded $LiCoO_2$ surface. After storage, electrolyte oxidation is suppressed on the repaired surface films due to its passivating ability, while it suffers from self-

discharged capacity during high temperature exposure, due to surface film repairing. Repaired surface films are similar to that of before storage. (3) Finally, CuO, a HF scavenger, suppresses degradation of surface films of LCO electrode. Charge capacity after storage, and capacity loss during storage are mitigated.

Keywords : $LiCoO_2$ electrode; Moderately elevated temperature; Surface films; Degradation; Repair; Hydrogen fluoride

Student number : 2014-30294

Contents

Abstract i

Contents v

List of figures viii

List of tables xiii

1 Introduction 1

2 Background 6

2.1 Electrochemical cells 6

2.2 Lithium−ion batteries 7

2.2.1 Definition and properties 7

2.2.2 Positive electrode 8

2.2.3 Negative electrode 10

2.2.4 Electrolyte 11

2.2.5 Surface film (electrode−electrolyte interface) 13

3 Experimental 15

3.1 Electrode and cell preparation 15

3.2 Electrochemical experiments 15

3.3 Reactive species (HF and PF_5) contact experiment 19

3.4 Measurement of dissolved materials in electrolyte 19

3.5 Spectroscopic investigations of surface film on the electrode..... 20

4 Results and discussion 23

4.1 Degradation of surface film on $LiCoO_2$ electrode by hydrogen fluoride attack at moderately elevated temperature. 23

4.1.1 Formation of surface films on LCO electrode through pre-cycling 23

4.1.2 Degradation of surface films on LCO electrode during storage at moderately elevated temperature 28

4.1.3 Unraveling the degradation mechanism of surface films 37

4.2 Behavior of surface film at higher State-Of-Charge (SOC) at moderately elevated temperature and its effect on cell performance 46

4.2.1 Degradation and repairing of surface films at moderately elevated temperature at its effect on cell performance 46

4.2.2 Identification of repaired surface films using spectroscopic experiments 56

4.2.3 Effect on the degradation of the full-cell 62

4.3 A countermeasure to mitigate cell degradation at moderately elevated temperature: HF scavenger (cupper(II) oxide, CuO) addition into LCO electrode to suppress surface film degradation 65

4.3.1 Effect of CuO on surface film degradation and cell performance degradation 65

4.3.2 Spectroscopic analysis of surface films on CuO-added LCO electrode 71

5 Conclusion 74

References 76

국문초록 89

List of figures

Figure 1 Experimental scheme to simulate exposure to high temperature 17

Figure 2 Experimental scheme to simulate exposure to high temperature with various SOC cells 18

Figure 3 Scheme for reactive species (HF and PF_5) contact experiment 22

Figure 4 XPS spectra of $LiCoO_2$ electrode (a) before and (b) after pre-cycling (10 charge/discharge cycles) 25

Figure 5 Field emission microscope image of $LiCoO_2$ composite electrode surface after pre-cycling. The marked squares denote the sites of AES measurement 26

Figure 6 TEM images of $LiCoO_2$ particles (a) before and (b) after pre-cycling. The surface film thickness is indicated by arrows 27

Figure 7 Evolution of charge and discharge specific capacity of Li/$LiCoO_2$ cells before and after storage. The cells were "pre-cycled" 10 times at 25 °C, and then stored at (a) 25, (b) 60, or (c) 70 °C for 10 h. The cells were then "re-cycled" at 25 °C. The Coulombic efficiency is compared in (d). Current density: 0.1 *C*, voltage cutoff: 3.0–4.3 V (*vs.* Li/Li^+). 32

Figure 8 Change of open-circuit voltage (OCV) of Li/LCO cells during the elevated-temperature storage. 33

Figure 9 Current and discharge specific capacity of Li/LCO cell traced after a cell voltage of 2.8 V is intentionally imposed to simulate the final stage of 70 ° C storage (Fig. 8). 34

Figure 10 Supposed mechanism of degradation of surface films on LCO electrode and degradation of cell performance of Li/LCO cell at moderately elevated temperature 35

Figure 11 Coulombic efficiency and specific capacity of Li/LCO cell using fresh LCO and Li metal, and electrolyte solution collected after 70 ° C storage 36

Figure 12 XPS spectra obtained from $LiCoO_2$ electrode surface (a) before storage (pre-cycled), (b) after storage at 70 ° C for 10 h in the standard electrolyte (1.3 M $LiPF_6$ in EC/DEC), (c) after storage at 70 ° C for 10 h in EC/DEC with 400 ppm added HF, and (d) after exposure to PF_5(g) for 10 h. 41

Figure 13 . (a) Variations of charge/discharge specific capacity and Coulombic efficiency of Li/$LiCoO_2$ cells before and after 70 ° C storage. The electrolyte was 0.5 M $LiPF_6$ in EC/DEC (3/7, v/v), and other experimental conditions were the same as for Fig. 7c. (b) Comparison of OCV decay for the two Li/LCO cells (with 0.5 and 1.3 M $LiPF_6$ in the electrolyte) traced during 70 ° C storage. 42

Figure 14 Atomic percentages of the elements in the surface films derived from XPS spectra. Three samples were compared: pre-cycled LCO electrode (before storage), after 70 ° C storage in

the standard electrolyte, and after 70 ° C storage in EC/DEC with 400 ppm added HF. 43
Figure 15 TEM images of (a) pre-cycled LCO, (b) after 70 ° C storage in the standard electrolyte, and (c) after 70 ° C storage in EC/DEC with 400 ppm added HF. 44
Figure 16 SEM images of the LCO electrodes (a) before and (b) after storage at 70 ° C in the standard electrolyte. (c) and (d) are magnified images of (a) and (b). 45
Figure 17 OCV profiles of Li/LCO cells of various SOCs during storage at 70 °C. After 10 h of storage, they are divided into two groups by remaining SOC (Red and blue box each). 50
Figure 18 The graph illustrating how to measure self-discharged capacity during storage 51
Figure 19 Coulombic efficiencies of the cells before and after storage at 70°C for 10 h 53
Figure 20 Charge and discharge capacities of the SOC0 cell and the SOC50 cell (data of the SOC0 cell is the same as Fig. 7c). 54
Figure 21 Voltage profiles of the SOC0 cell and the SOC50 cell before and after storage 55
Figure 22 XPS spectra of surface films on LCO electrodes at SOC50 before and after storage at 70 °C 58
Figure 23 Atomic ratio of the LCO electrodes calculated from XPS result. Before and after storage at 70 °C of the SOC0 cell and the SOC50 cell 59

Figure 24 SEM images of LCO electrodes of the SOC50 cell (a) before and (b) after storage at 70 °C. TEM images of surface films on LCO electrodes of the SOC50 cell (c) before and (d) after storage at 70 °C. 60

Figure 25 Schematic illustration of surface film behaviors of the electrodes of the two groups and effects on the cells during and after storage 61

Figure 26 Schematic diagram of capacity loss of full-cell during storage at 70 °C, when LCO electrode is charged before storage 63

Figure 27 Schematic diagram of capacity loss of full-cell during and after storage at 70 °C, when LCO electrode is discharged before storage. 64

Figure 28 OCV plots of CuO-free and CuO-added Li/LCO cell during storage at 70 °C (Data of the CuO-free cell is same as the data of Fig.8) 68

Figure 29 Charge and discharge capacities and Coulombic efficiencies of CuO-free and CuO-added cells. They are stored at 70 °C for 6 h after 10 cycles of pre-cycling. 69

Figure 30 C 1s, O 1s and F 1s XPS spectra of CuO-added LCO electrode before and after storage at 70 °C 72

Figure 31 SEM images of CuO-added LCO electrode (a) before and (b) after storage at 70 °C. TEM images of surface films on

CuO-added LCO electrode (c) before and (d) after storage at 70 °C 73

List of tables

Table 1 Self-discharged capacities of the cells during storage at 70 °C for 10 h 52

Table 2 Self-discharged capacities of CuO-free and CuO-added Li/LCO cells during storage at 70 °C for 10 h. (Data of CuO-free cell is the same as the data of Table 1) 70

1 Introduction

Lithium-ion batteries (LIBs) are currently ubiquitous in electronic devices and electric vehicles for energy conversion and storage, due to their better performance than other candidates. Presently, the most popular cell components for LIBs are graphite or silicon for the negative electrode, lithium metal oxides of layered or spinel structure ($LiMO_2$, M = Co, Ni, or Mn; and LiM_2O_4, M = Ni or Mn) for the positive electrode, and $LiPF_6$-containing organic carbonate solvents as the electrolyte.

Frequently, LIBs are exposed to moderately elevated temperature (ca. 60-100 °C) through either heavy-duty use or abuse. Unfortunately, LIBs fabricated with these cell components can be degraded at this temperature, which shortens the cell life or triggers safety problems [1-4]. Hence, it is very important to unravel the failure mechanisms of LIBs in this temperature range and explore the appropriate countermeasures. Obviously, many components of the typical cells cannot be thermally degraded at 60-100 °C, such as the positive or negative active materials themselves, carbon conducting agent, and metal current collector [5]. Rather, the thermal generation of some reactive chemical species inside the cells and their attack on cell components are the more likely causes according

to literature reports [6−11]. In particular, hydrogen fluoride (HF) as a reactive species should be considered, since it is easily generated via several routes. It is generated by the hydrolysis of $LiPF_6$ [12]. Above 60 ° C, the thermal decomposition of $LiPF_6$ generates PF_5 [13, 14], which further generates HF by reactions with either impurity water [15−17] or diethyl carbonate (DEC) of electrolyte [18−20]. Several undesirable effects from the as−generated HF have been reported [6−10]. For example, the $LiCoO_2$ (LCO) positive electrode can be attacked by HF to cause Co dissolution, and the dissolved metal ions are transferred to and plated on the negative electrode to cause self−discharge or cell degradation [6−8]. HF can also corrode the metal current collectors [9] and degrade the electrolytes [10, 21].

In the present LIBs, some amounts of electrolytes are inevitably reduced/oxidized at the negative/positive electrodes under the cell working conditions, leaving surface films on the electrode surfaces [22−26]. Fortunately, the surface films are electrically insulating, so that further electrolyte reduction/oxidation is prevented due to the passivating role of the surface films [22, 23]. To achieve the best passivating ability, the surface films should be uniform, fully cover the electrode surface, and thicker than the electron tunneling length. When the surface film on the negative electrode is damaged to lose its passivation ability, electrolyte can decompose on the damaged

areas and deposit new film to repair the damaged surface film. This process leads to capacity fading and eventually shortened cell life, and sometimes it triggers thermal runaway processes due to heat evolution [27−29]. Compared to the negative electrodes, the study of surface films on positive electrodes of LIBs (for example, LCO) is rather limited. Nevertheless, the generation mechanisms and the chemical compositions of the surface films on positive electrode have been reported [24, 26, 30−33]. Given that these films contain both inorganic (LiF and Li_2CO_3) and organic (oligomers such as Li alkyl carbonates and polymers such as polycarbonate and polyethylene) species, it is very likely that the surface films on positive electrode are vulnerable to HF attack so as to the surface films on negative electrode [34, 35].

Based on the context discussed above, the first part attempts to answer the following questions: (i) whether the surface film on the LCO positive electrode is degraded upon exposure to moderately elevated temperature, (ii) if yes, whether the degradation is caused by the attack of reactive species such as HF, and (iii) how the film degradation affects the cell performances.

Based on the result of part 1, in the second part, behavior of surface films at moderately elevated temperature of higher state−of−charge (SOC) cell, and its effect on cell performance are studied. In a practical situation, it is more common for a battery to be exposed to

high temperature in charged state. If surface films on LCO electrode is degraded and lose its passivating ability, electrolyte is oxidized on the naked LCO electrode leaving surface films on it (surface film repairing) reducing LCO, when there are vacant Li^+/e sites in LCO. Oxidation of the electrolyte would be continued until the cell becomes SOC0. Repaired surface film is generated by electrolyte oxidation, and its composition would be similar with that after pre-cycling. So, passivation ability of repaired surface film after storage is expected to be similar to that before storage. Objectives of the second part are to reveal following things; (i) whether surface film is repaired on the degraded LCO electrode during storage at moderately elevated temperature, when the cell SOC is higher than 0, and (ii) if yes, how the behavior of surface films affects cell performance.

In the third part, based on the result of part 1 and 2, to suppress cell degradation, it is tried to reduce HF, the cause of surface film degradation at elevated temperature. As a countermeasure, CuO is added into LCO electrode. CuO was reported as HF scavenger since CuO reacts with HF generating $CuF_x \cdot H_2O$ moiety [36]. Objectives of part 3 are to answer following questions; (i) whether CuO in the LCO electrode mitigates degradation of surface film of LCO electrode, and (ii) if yes, how it alleviates the degradation of Li/LCO cell at moderately elevated temperature.

To this end, a Li/LCO cell is fabricated and cycled with 0.1 *C* in 3.0–4.3 V (*vs.* Li/Li^+) voltage range to deposit surface films on the LCO surface, and then stored at moderately elevated temperatures (60 or 70 ° C) for 10 h to simulate the high–temperature exposure. In part 1, Li/LCO cell of SOC0 is stored to investigate the degradation of surface film. In part 2, the cells of five different SOCs of somewhat similar open–circuit voltages (OCVs) are stored at 70 °C to examine the effect of higher SOC on cells. After the storage, the cells are cycled again at 25 ° C and investigate any change (degradation) of cell during storage compared to before storage. Postmortem analyses are performed on the damaged (stored) LCO electrodes. In part 3, Li/LCO cell are prepared using CuO–added LCO electrode, and the same experiment as above is performed.

2 Background

2.1 Electrochemical cells

Electrochemistry studies the relationship between electricity and chemical change. The change of Gibbs free energy is converted to electrical potential as below.

$$\Delta G = -nFE$$

Electrochemical cell is a device generating electrical energy from chemical energy. It basically consists of working electrode and counter electrode. When oxidation (reduction) reaction occurs on the working electrode, reduction (oxidation) reaction occurs on counter electrode, and electrons are transferred through circuit, making closed loop. One of the two electrodes where oxidation occurs is called anode, and the other is called cathode. The voltage of a cell is difference of potential of anode and potential of cathode as below.

$$E_{cell} = E_{anode} - E_{cathode}$$

In an ‘electrolytic cell’, energy is supplied from external power supply and nonspontaneous reactions ($\Delta G>0$) occur on the anode/cathode. As a result, the electrical energy is converted and stored in the cell in chemical energy form. In a ‘galvanic cell’, spontaneous reactions ($\Delta G<0$) occur on the anode/cathode, and

chemical energy stored in the cell is converted to electrical energy. Electrolyte is filled between anode and cathode. Ion salts are dissolved in electrolyte to transport ions, but electrolyte is electrical insulating (electrons are transported through external circuit). When the stored chemical energy is used to electric energy, it is called ‘discharge’. When the cell is supplied electrical energy from external power, it is called ‘charge’. The secondary battery is a cell capable to be charged and discharged. When the secondary battery is charged, the positive electrode is oxidized (anode) and the negative electrode is reduced (cathode). When it is discharged, the positive electrode is reduced (cathode) and the negative electrode is oxidized (anode). Because it is somewhat confusing, the positive/negative electrode is more useful rather than cathode/anode for secondary battery.

2.2 Lithium-ion batteries

2.2.1 Definition and properties

Lithium-ion battery (LIB) is one of the most used secondary battery, in these days, because LIB has the advantage of light weight and large capacity[37]. It is composed of positive and negative electrode which can insert or extract lithium ions, and electrolyte in which lithium ions

are dissolved. During discharge, lithium ions are transferred from positive electrode to negative electrode through electrolyte, and vice versa during charge. Therefore, it is also called 'rocking chair battery'. Representative reaction equations are as below;

Positive electrode: $\mathrm{LiCoO_2} \leftrightarrow Li_{1-x}CoO_2 + xLi^+ + xe$

Negative electrode: $C_6 + xLi^+ + xe \leftrightarrow Li_xC_6$

It was firstly commercialized in 1990 in Japan, and its market is growing into mobile devices, power tools, electric vehicles, and energy storage systems.

2.2.2 Positive electrode

$LiCoO_2$ (O3−type, rhombohedral, LCO) is one of the most famous active material for positive electrode. When LCO is discharged, Li^+ is extracted from LCO and Co is oxidized from Co^{3+} to Co^{4+}.

$$\mathrm{LiCoO_2} \underset{Discharge}{\overset{Charge}{\rightleftharpoons}} xLi^+ + xe + Li_{1-x}CoO_2$$

The theoretical specific capacity of the $LiCoO_2$ is about 273 mA h g^{-1} and calculated as below.

Specific capcity [mA h g^{-1}]

$$= \frac{(number\ of\ Li\ ) \times 96500\ \left[\frac{C}{eq}\right] \times 1000\ \left[\frac{mA}{A}\right]}{(Molecular\ weight\ of\ active\ mateial) \left[\frac{g}{mol}\right] \times 3600 \left[\frac{s}{h}\right]}$$

$$= \frac{1 \times 96500 \times 1000}{98\ \times 3600} = 273$$

Structure of LCO changes as lithium is extracted [38]. The structure is stable in the range of 0<x<0.5. When x is over ca. 0.5, the structure becomes collapsed. When the structure is collapsed, lithium is hard to be extracted or inserted into the structure. When 0.5 Li is extracted from LCO, specific capacity is about 150 mA h g^{-1}, and voltage upper cut-off is ca. 4.3 V (vs. Li/Li^+), and the average voltage is ca. 3.7 V (*vs.* Li^+/Li). Doping or coating techniques are useful to suppress the structure collapse, and makes capacity and life of LCO larger and longer.

$LiNi_{1-x-y}Co_xAl_yO_2$ (NCA) is one of promising active material for positive electrode due to its larger specific capacity than that of LCO. Since NCA has slightly lower redox potential than LCO, capacity of NCA is larger than LCO in the voltage range under 4.3 V (*vs.* Li/Li^+) [39]. Size of Ni^{2+} is similar with Li^+, and site exchange between Li^+ and Ni^{2+} easily occurs, making capacity of NCA decrease and resistance increased. When Li^+ is extracted, its structure is transformed to rock-salt structure, of which Li^+ insertion/extraction is blocked [40, 41]. This is especially progressed from surface of NCA particles. Doping of Al into NCA helps the structure and capacity

preserved[42]. Mixed transition metal with Mn and Co also helps the structure preserved.

Spinel type of positive active material, $LiMn_2O_4$ (LMO) is also invented and used. It has faster Li^+ kinetics but lower specific capacities than LCO. It suffers from Mn dissolution due to Jahn-teller distortion and HF attack[43]. $LiMn_{0.5}Ni_{1.5}O_4$(LNMO) has relatively stable structure than LMO, and higher redox potential (4.5~5.0 V (*vs.* Li/Li^+)) than LMO[44, 45], so it is merit on energy density and stability of active material itself.

2.2.3 Negative electrode

Before convention of lithium ion secondary battery, primary battery which can be discharged only has lithium metal as negative electrode. Li has merit on theoretical energy density because Li has large specific capacity (3,860 mA h g^{-1}) and low redox potential (−3.04 *V* (vs. NHE)). The limit of Li metal as negative electrode for secondary battery is dendrite growth when it is lithiated (i.e. charged), and dead lithium generation as a result of volume shrinkage/expansion and surface film generation making cell capacity degraded[46].

Carbonaceous materials have been most used as negative electrode active materials, due to their cheap cost, stability, and low redox

potential[47]. Graphite is one of the most used carbonaceous material for negative electrode. It has low redox potential close to that of Li and ca. 360 mA h g^{-1} capacity[48]. Li is intercalated into Li^+/e site in graphite to make LiC_x. There are natural and artificial graphite. There are also soft carbon and hard carbon. Their capacities are smaller than that of graphite, because their disordered structure, but their rate capability can be better than that of graphite due to the structure.

Silicon has been studied as post graphite negative electrode material, because it has larger capacity than graphite (theoretically, 4,200 mA h g^{-1}). As it is lithiated generating $LiSi_x$ alloy, its volume expansion is larger than graphite[49, 50]. To take advantage of the large capacity, Si is used as a mixture with graphite materials, today. Other alloy type materials such as Sn, and Sb have been also studied.

2.2.4 Electrolyte

Electrolyte is composed of solvents including Li salt. They have to chemically and electrochemically stable in using voltage range and temperature. To get wide electrolyte stable window, aprotic solvent is used rather than water, nowadays. To obtain appropriate melting/boiling point, viscosity, and dielectric constant, mixtures of

linear and ring type carbonates are often used. Ring types have high dielectric constant and easily dissolve Li salts. Linear types have low viscosity, making Li^+ more mobile.

The lithium salts of electrolyte for lithium ion battery should be easily dissolved in the electrolyte solution, chemically and electrochemically stable and free from corrosion. Lithium hexafluorophosphate ($LiPF_6$) is commonly used Li salt. It is well dissolved in carbonates and dissociated to Li^+ and PF_6^-. It passivates Al from Al corrosion making AlF_3 passivating layer during oxidation [51]. One severe drawback is its decomposition. It reacts with water[52], and makes HF at room temperature. It is decomposed to LiF and PF_5 over 60 °C. PF_5 is Lewis acid, and reacts with Lewis base such as electrolyte [20] or water, and generate HF. HF is a reactive material that corrode organic, inorganic materials [53, 54]. It corrodes other components of cells, for example, current collector and active materials [53]. When HF is released from the battery, it causes health problems for the users [55].

Additives of the electrolyte are used to improve cell performances, such as thermal stability [56], low temperature performance [57], cycle life [58, 59], and over-charge properties [60] by improving passivating ability or durability of surface films of the electrode, or scavenging reactive species.

2.2.5 Surface film (electrode–electrolyte interface)

In today's LIBs, operating voltage range exceeds the LUMO (or HOMO) of the electrolyte, so the electrolyte is inevitably oxidized/reduced on the positive/negative electrode. Byproducts of the electrolyte are deposited on the electrode generating films. They are electrically passivating, and suppress additional electrolyte decomposition on it. Well–made surface films are effective for cell energy efficiency, cycle life, and resistance.

Surface films are very complicated because they are composed of many materials. Surface films of the negative electrode, called 'Solid–Electrolyte–Interphase (SEI)', are composed of mixture of inorganic materials (LiF, Li_2CO_3) and organic materials (oligomer such as LiOCOOR, $(CH_2OCO_2Li)_2$), polymer (polycarbonate)) like mosaic [23].

Surface films of the positive electrode is not studied as much as SEI, because (1) it is thinner and less than SEI so it is difficult to analysis, and (2) positive electrode is not exfoliated like graphite of the negative electrode by electrolyte[26]. Nevertheless, When carbonate–based electrolyte is used together with $LiPF_6$ salt, the surface film of the $LiCoO_2$ electrode is generated through about three step[26]. The first is native film, Li_2CO_3, generated on $LiCoO_2$ active

material as a residue of precursor of synthesis process or during storage in ambient air atmosphere as a result of reaction between $LiCoO_2$ and CO_2 [31, 61]. Next, during soaking in electrolyte, native Li_2CO_3 on its surface is dissolved in electrolyte [62] and/or converted to LiF and gaseous material as a result of a reaction with HF dissolved inevitably in electrolyte [31]. The electrolyte is also spontaneously oxidized leaving LiOCOOR or LiOCO on the electrode by nucleophilic attack to $LiMO_2$ (M=Ni, Co) [62, 63]. During charging, as a final, Li poor alkyl carbonate, polycarbonate, polyethylene or oligomers, which are carbonate-based electrolyte oxidized decomposition materials, are generated [64]. Salt decomposed materials, $Li_xPF_yO_z$ and LiF, are also exist.

3 Experimental

3.1 Electrode and cell preparation

The composite electrodes were prepared from a slurry of LCO (KD10, Umicore), carbon conducting agent (Super P, Timcal), and polyvinylidene fluoride (PVdF, solef 6020, Solvay) (90:5:5 in wt. %) in N-methyl-2-pyrrolidone (NMP, Sigma-Aldrich). The slurry was coated on Al foil with a doctor blade (loading amount: ca. 0.3 mA h cm^{-2}), and then pressed and dried at 120 ° C in a vacuum overnight. CuO-added electrode was made with the slurry of LCO, CuO (sigma-aldrich, < 50nm), carbon conducting agent, and PVdF (88:2:5:5 in wt. %) with same method with CuO-free electrode.

Two-electrode 2032-type coin-cells (Hoshen) were assembled with the as-prepared LCO composite electrode, separator (polypropylene/polyethylene/polypropylene, PP/PE/PP, Celgard), and Li metal. The electrolyte was 1.3 M $LiPF_6$ in ethylene carbonate (EC)/diethylene carbonate (DEC) (30:70 in vol. %, Panax etec).

3.2 Electrochemical experiments

After cell assembly, the first step was "pre-cycling", i.e., galvanostatic charge/discharge cycling at 0.1 *C* (15 mA g^{-1}) at 25 °C for 10 cycles in the potential range of 3.0–4.3 V (*vs.* Li/Li^+) using a battery cycler (TOSCAT 3100, Toyo Co.). A rest period (10 min) was added between the cycles, and a constant voltage step was added in the charging period until the current decayed down to 0.01 *C* (1.5 mA g^{-1}). In the second step, the pre-cycled cells were stored at moderately elevated temperature (60 or 70 °C) for 10 h. Before the storage, the Li/LCO cell was discharged down to 3.0 V to adjust the state-of-charge (SOC) of LCO electrodes to zero and rested for 1 h. After storage, charge/discharge cycling at 25 °C (referred to as "re-cycling") was performed at the same condition as for the pre-cycling, in order to examine possible cell failure due to the storage.

For storage test of various SOC cells, after pre-cycling, the cells were charged to SOC5, 10, 25 or 50 (SOC100=150 mA h g^{-1}) with constant current (0.1 *C*, 15 mA g^{-1}), left for 1 h at 25 °C, and stored at 70 °C. After storage, the cells were discharge to 3.0 V (*vs.* Li/Li^+) with constant current (0.1 *C*, 15 mA g^{-1}) and re-cycled (charge/discharge cycling as same above) at 25 °C.

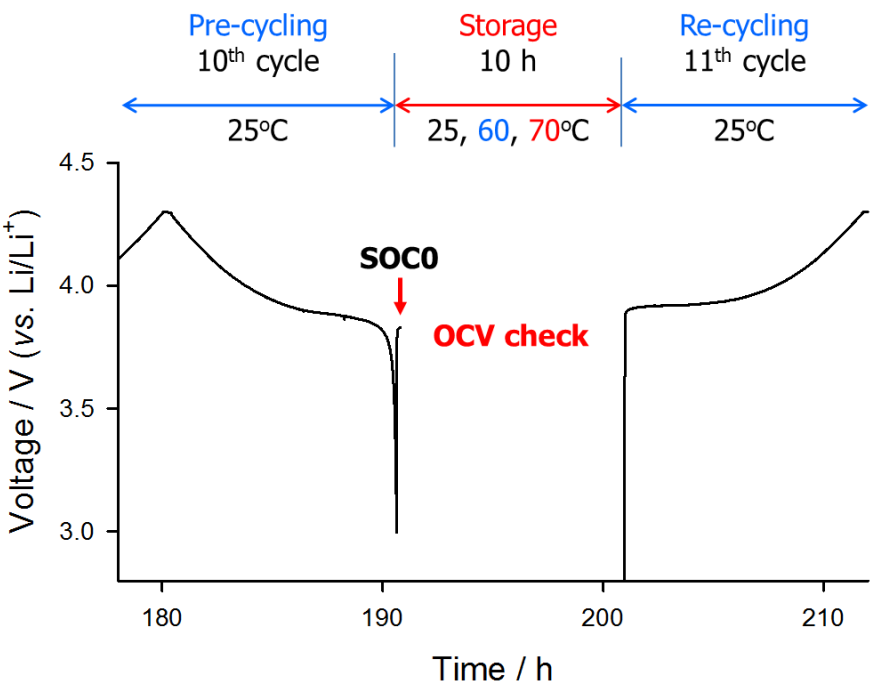

Figure 1 Experimental scheme to simulate exposure to high temperature

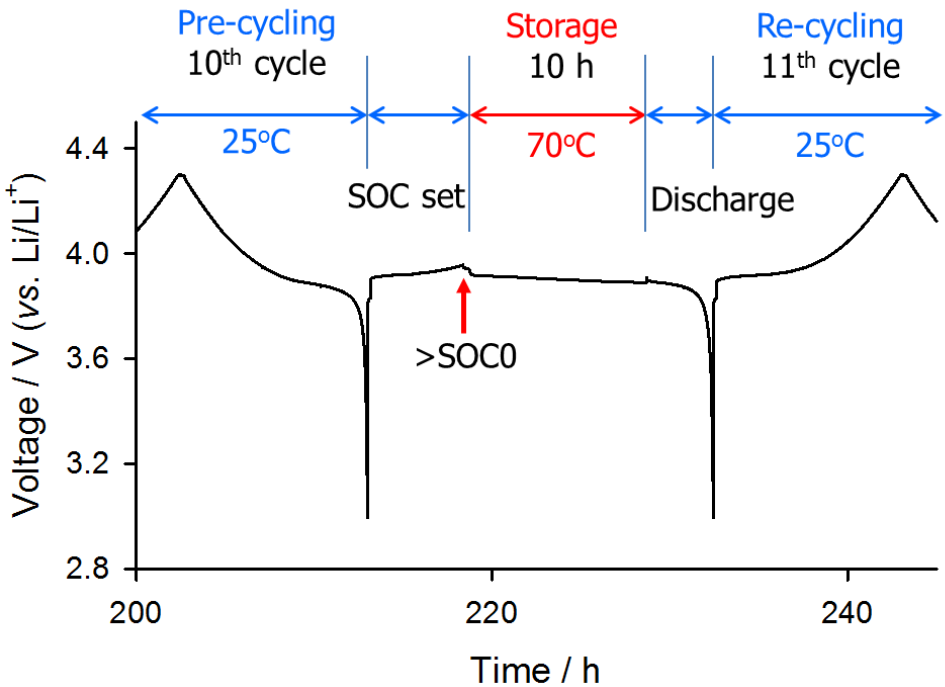

Figure 2 Experimental scheme to simulate exposure to high temperature with various SOC cells

3.3 Reactive species (HF and PF_5) contact experiment

To confirm possible HF attack on the surface films, an HF contact experiment was also performed. To this end, the pre-cycled (surface-film deposited) LCO electrodes were immersed in EC/DEC (30:70 in vol. %) containing HF (400 ppm) and stored at the same condition (70 ° C for 10 h). Note that $LiPF_6$ was not added to the solution in this experiment. To simulate possible PF_5 attack on the surface films, a flask containing $LiPF_6$ was heated at 70 ° C to produce PF_5 gas, and the gas was transferred to another flask containing the pre-cycled LCO electrode heated at 70 ° C (to simulate the storage at elevated temperature) [30].

3.4 Measurement of dissolved materials in electrolyte

The HF concentration in the electrolytes was measured by titrating with 0.01 N NaOH solution with an 888 Titrando titrator (Metrohm). The dissolved metal ion contents in the electrolyte solutions were

analyzed by using inductively-coupled plasma mass spectrometry (ICP-MS, NexION 350D, Perkin-Elmer). For measurement, after storage, the coin-cell was disassembled carefully and all parts were washed with DEC to avoid loss of electrolyte in the cell. Sampled DEC solution was used as ICP sample. All processes were carried out in an Ar-filled glove box. Obtained raw data was changed to concentration (unit of ppm) to the active material quantity of the electrode by calculating.

3.5 Spectroscopic investigations of surface film on the electrode

X-ray photoelectron spectroscopy (XPS, Sigmaprobe, UK) experiment was performed using Al Kα (1486.6 eV) radiation (15 kV, 10 mA) with a spot radius of ca. 200 μm. In an Ar-filled glove box, the sample electrodes were collected by disassembling the stored cells, washed with DEC, and dried under vacuum. For careful washing, the electrodes were immersed in DEC for a few minutes and then gently shaken. The binding energy was calibrated with the C 1s peak (285.0 eV). The atomic concentration of any element x in the sample, C_x, was calculated using the following equation [38, 39].

$$C_x(\%) = \frac{I_x/S_x}{\sum I_i/S_i} \times 100$$

Where I_i is the number of photoelectrons per second detected from the analysis volume for atom species i, Si is the atomic sensitivity factor, and I_x and S_x are the corresponding values for the element x. Fitting the XPS data and calculation of atomic concentrations were performed by Thermo Avantage software.

Auger electron spectroscopy (AES, PHI700Xi, Physical Electronics) was conducted at 0° of tilt with an electron gun analyzer (10 keV, 10 nA) and a square-shaped spot 1-2 μm along the edge. The sample preparation and atomic ratio calculation were the same as those for the XPS measurements.

Transmission electron microscopy (TEM, JEM-2100F, JEOL) analysis was performed at 200 kV. To prepare the sample, the composite electrode was carefully scraped from Al foil in an Ar-filled glove box. The obtained powder was dispersed in DEC by sonication, dropped onto lacey C-coated Cu grid, and dried under vacuum overnight. Surface images were observed using Scanning Electron Microscope (SEM). The electrodes were prepared with the same method for the XPS experiment. The electrodes were obtained from disassembled cell and washed with DEC and dried under vacuum overnight.

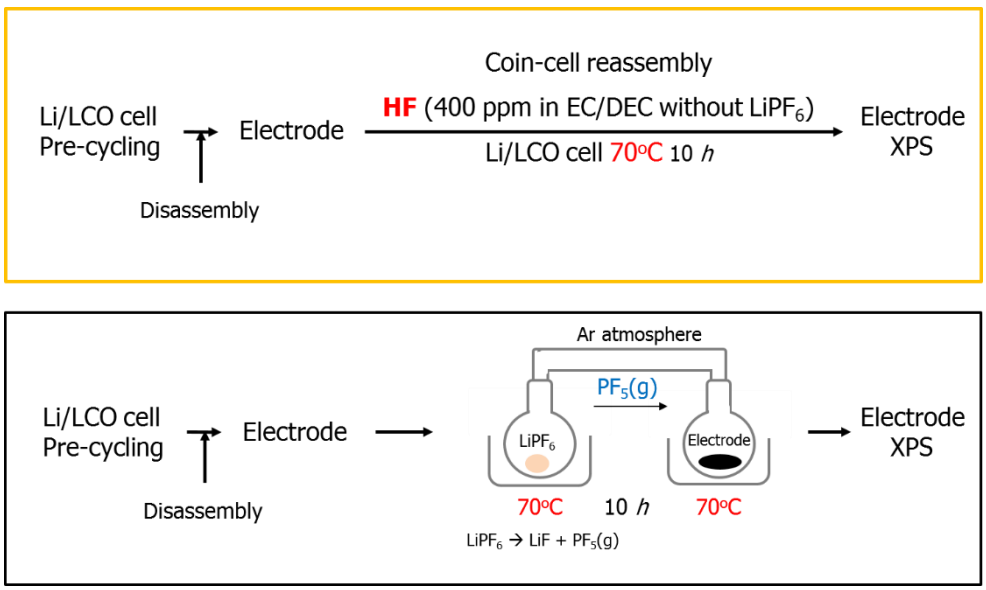

Figure 3 Scheme for reactive species (HF and PF_5) contact experiment

4 Results and discussion

4.1 Degradation of surface film on $LiCoO_2$ electrode by hydrogen fluoride attack at moderately elevated temperature

4.1.1 Formation of surface films on LCO electrode through pre-cycling

Fig. 4 shows the XPS spectra obtained from the fresh LCO composite electrode. The photoelectron peaks could be assigned to LCO (530 eV in O 1s and 780.6 eV in Co $2p_{3/2}$) [65] and PVdF binder (286.5 and 291.1 eV in C 1s, and 688 eV in F 1s) [66]. Photoelectrons emitted from Li_2CO_3 (290.0 eV in C 1s and 532 eV in O 1s) were also detected, which may be formed on LCO during the synthesis or storage in ambient atmosphere as a result of reaction with CO_2 [31, 61]. LiF (685 eV in F 1s) was also detected, as the reaction product between LCO or Li_2CO_3 on the powder surface and hydrofluoric acid produced during the electrode fabrication process [31]. The XPS data in Fig. 1b reveal that the peaks of C-O (286.5 eV), C-O-C and C=O (287.8 eV), O=C-O (289.0 eV), and CO_3 (290.6 eV) in the C 1s spectra [67], and those of C=O and CO_3 (532 eV) and C-O (533.5 eV) in the O 1s spectra [31, 68] became more

intense after the pre-cycling, at the expense of the peak from the lattice oxygen of LCO (532 eV in O 1s). Note that the only source of all these C- and O-containing chemical species is the solvent molecules in the electrolyte, illustrating that the surface film was deposited by oxidative decomposition of the electrolyte solution. To confirm the surface film deposition, AES measurement was made on the marked squares of ca. 1-2 μm in size on the surface of pre-cycled LCO particle (Fig. 5). Note that the Auger electrons were detected only from the squared spots to avoid the contribution from conductive carbon. The average atomic composition in the squared spots was C 36%, O 24%, Co 13%, and trace amounts of P and F; clearly indicating that the LCO surface was covered by carbon- and oxygen-containing species that must be derived from the carbonate solvents [31]. The TEM image taken before pre-cycling shows that a surface film <1 nm in thickness was deposited during the composite electrode preparation step (Fig. 6 (a)), and this film became as thick as 5 nm after pre-cycling (Fig. 6(b)). In short, a ca. 5-nm thick surface film containing carbon and oxygen species derived from electrolyte decomposition was deposited on the LCO surface during the pre-cycling.

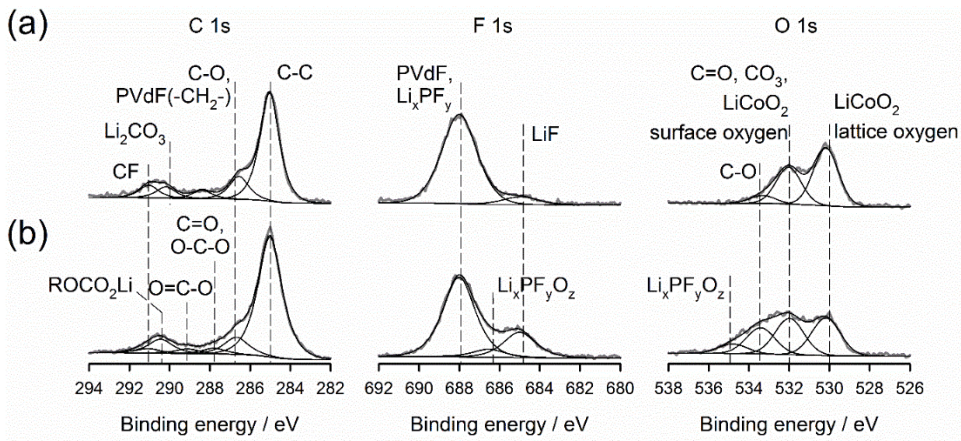

Figure 4 XPS spectra of $LiCoO_2$ electrode (a) before and (b) after pre-cycling (10 charge/discharge cycles)

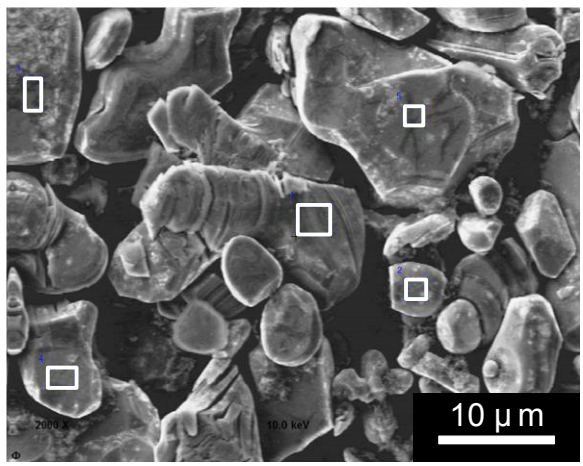

Figure 5 Field emission microscope image of $LiCoO_2$ composite electrode surface after pre-cycling. The marked squares denote the sites of AES measurement

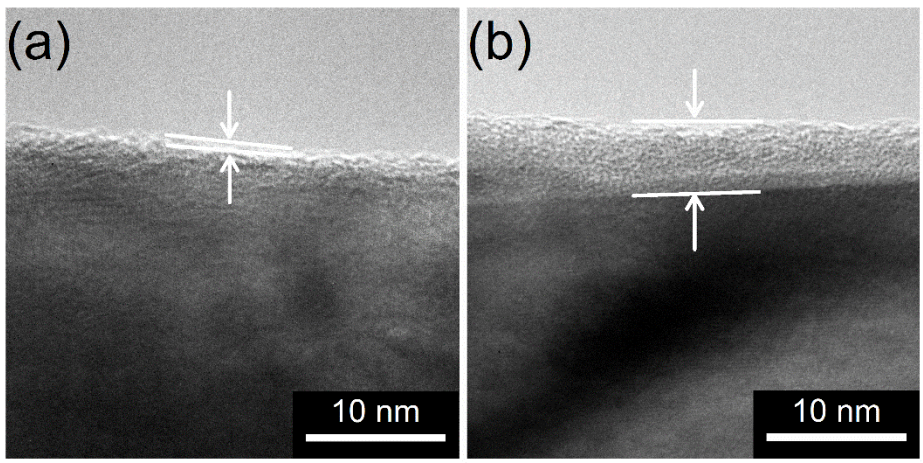

Figure 6 TEM images of $LiCoO_2$ particles (a) before and (b) after pre-cycling. The surface film thickness is indicated by arrows

4.1.2 Degradation of surface films on LCO electrode during storage at moderately elevated temperature

Figs. 7a-7c show the evolution of charge/discharge capacity of Li/LCO cells during the pre-cycling and re-cycling periods. Note that the re-cycling was carried out to examine any cell damages evolved during the storage. The specific discharge capacity (lithiation and the reduction of LCO electrodes) is about 150 mA h g^{-1} before the storage, which is largely unchanged after the 70 ° C storage (Fig. 7c). Therefore, the bulk properties of LCO, which affect the electrode capacity, are not seriously changed upon exposure to the elevated temperature. Moreover, the Co dissolution from LCO during the 70 ° C storage (measured to be 140 ppm, or 0.02 % of the Co in LCO) is not large enough to affect the electrode capacity. A notable difference, however, was that the charging capacity (de-lithiation and the oxidation of LCO electrodes) in the first cycle of re-cycling increased most prominently after the 70 ° C storage. Consequently, the Coulombic efficiency in this cycle is poorer than that before the thermal storage, although it is restored back to the initial value from the second cycle on.

In order to examine changes of the cell during thermal storage, the open-circuit voltage (OCV) of Li/LCO cells was traced during the storage (Fig. 8). After placing in the storage, there was a rapid OCV

drop down to 2.8 V after some retention period, but this OCV drop was not appreciable at 25 or even 60 ° C. Note that 2.8 V is the OCV value of the fully discharged Li/LCO cell (fully lithiated for LCO electrode). The rapid OCV drop to 2.8 V means that the LCO electrode is reduced (fully lithiated) during the 70 ° C storage. Further, the appearance of a retention period illustrates that the LCO electrode, of which the SOC was assumed to be zero because it was fully discharged down to 3.0 V under the transient cycling condition, was not actually fully discharged (lithiated) [38]. To quantify this remnant capacity of LCO at SOC 0, the pre-cycled Li/LCO cell (OCV = 3.8 V *vs.* Li/Li^+) was intentionally discharged by the application of 2.8 V at 70 ° C (Fig. 7b) to match the final OCV and heated condition in Fig. 8, and the discharge current was obtained and converted to specific capacity. As shown in Fig. 9, the discharging (lithiation) capacity is 4 mA h g^{-1}, which means that the LCO electrode still has empty Li^+/electron co-injection sites (4 mA h g^{-1}) just before storage at the elevated temperature. However, these available co-injection sites are filled (lithiated) during the retention period, and then the OCV rapidly drops to 2.8 V (i.e., the fully lithiated state). Here, the lithiation (reduction of LCO electrode) should be accompanied by some oxidation process, which is tentatively assumed to be the electrolyte oxidation. [28, 69, 70]

The following scenario is proposed to explain what happens during the high-temperature storage. The surface film on the LCO electrode, formed during the pre-cycling, is damaged and loses its passivation ability. As a result, electrolyte oxidation occurs on the damaged LCO surface, and the deposited surface film repairs the damaged surface film. Both the undamaged and repaired surface film are vulnerable to damage when the cell is still stored at 70 °C. This film damage/repair process continues, until the empty Li^+/electron storage sites (4 mA h g^{-1}) are completely filled (i.e., the LCO electrode is fully lithiated). Once the LCO is fully lithiated (reduced or discharged), further repair is impossible, because electrolyte oxidation cannot take place without LCO reduction. Consequently, towards the end of the 70 °C storage, the damaged film remains unrepaired. Then, the LCO electrode with damaged film is charge/discharge cycled at 25 °C in the re-cycling period. In the first charging in re-cycling, the LCO electrode is charged (oxidized) from the fully discharged state, and electrolyte oxidation also takes place on the LCO surface exposed to the electrolyte solution due to film damage. The charges consumed for electrolyte oxidation are added to those consumed for lithiation (charging) of LCO electrode, so that the charging capacity appears to be larger than the normal value. Now, the damaged film is repaired during the first charging period as discussed above, but it is not damaged again because the cell is now at ambient temperature. Hence, there is no film

damage/repair in the rest of the re-cycling period, so that the higher Coulombic efficiency (>98%) is maintained from the second cycle on (Fig. 7d).

Another possible reason for the extra charging capacity of Li/LCO cell after 70 °C storage is the degradation of electrolyte solution by either salt decomposition or solvent decomposition [17]. Here, if one assumes that the degraded electrolyte solution is more prone to oxidation compared to the fresh one, the charging capacity in the first cycle of re-cycling will be larger than the normal value, because extra capacity from the electrolyte oxidation is added to the charging capacity of the LCO electrode. To check this possibility, the electrolyte solution was collected after the 70 °C storage, and loaded into a fresh Li/LCO cell and charge/discharge cycled. The result, shown in Fig. 11, illustrates that the obtained Coulombic efficiency and capacities are very similar to those obtained with the fresh electrolyte solution. Hence, the easier electrolyte oxidation due to thermal degradation is ruled out.

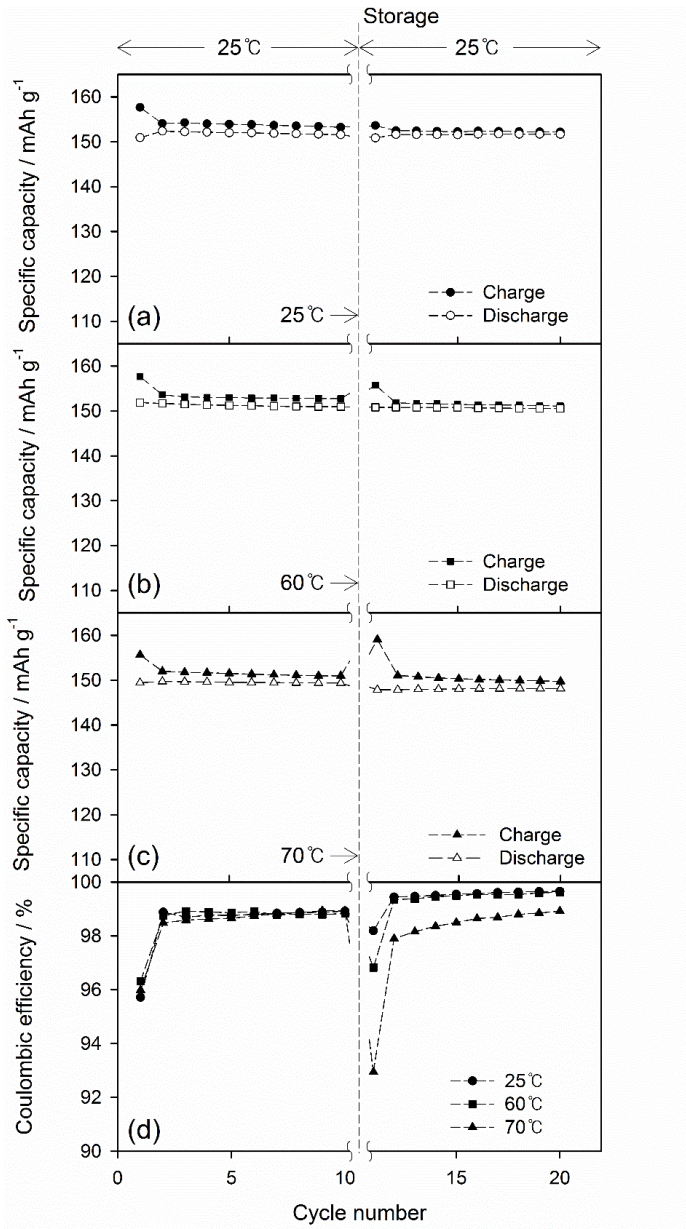

Figure 7 Evolution of charge and discharge specific capacity of Li/$LiCoO_2$ cells before and after storage. The cells were "pre-cycled" 10 times at 25 ° C, and then stored at (a) 25, (b) 60, or (c) 70 ° C for 10 h. The cells were then "re-cycled" at 25 ° C. The Coulombic efficiency is compared in (d). Current density: 0.1 *C*, voltage cutoff: 3.0-4.3 V (*vs.* Li/Li^+).

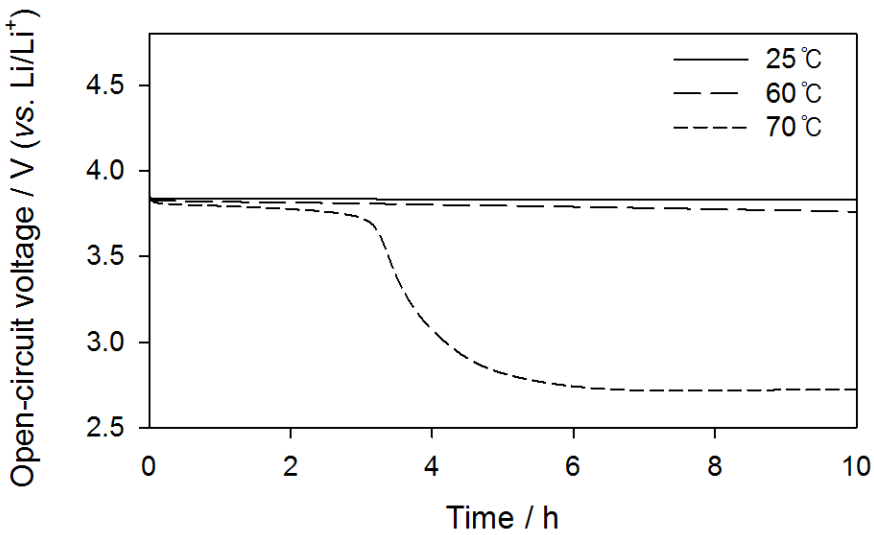

Figure 8 Change of open-circuit voltage (OCV) of Li/LCO cells during the elevated-temperature storage.

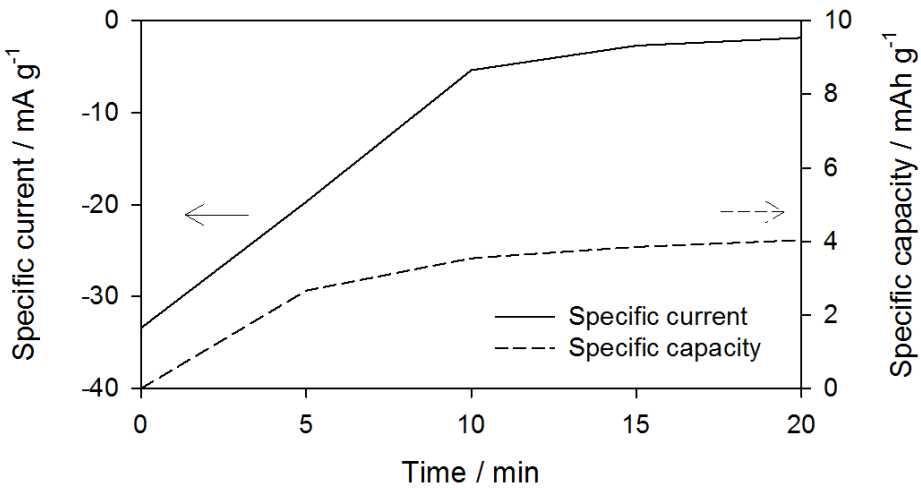

Figure 9 Current and discharge specific capacity of Li/LCO cell traced after a cell voltage of 2.8 V is intentionally imposed to simulate the final stage of 70 ° C storage (Fig. 8).

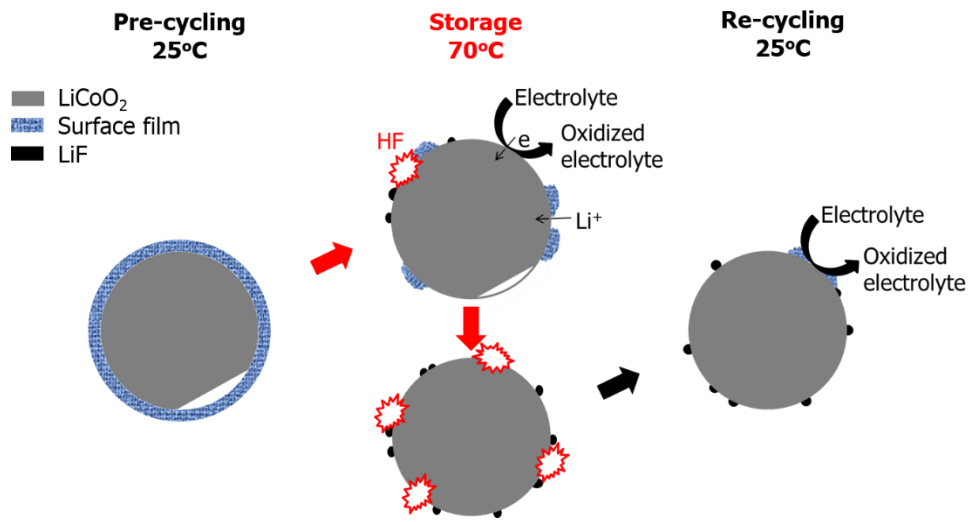

Figure 10 Supposed mechanism of degradation of surface films on LCO electrode and degradation of cell performance of Li/LCO cell at moderately elevated temperature

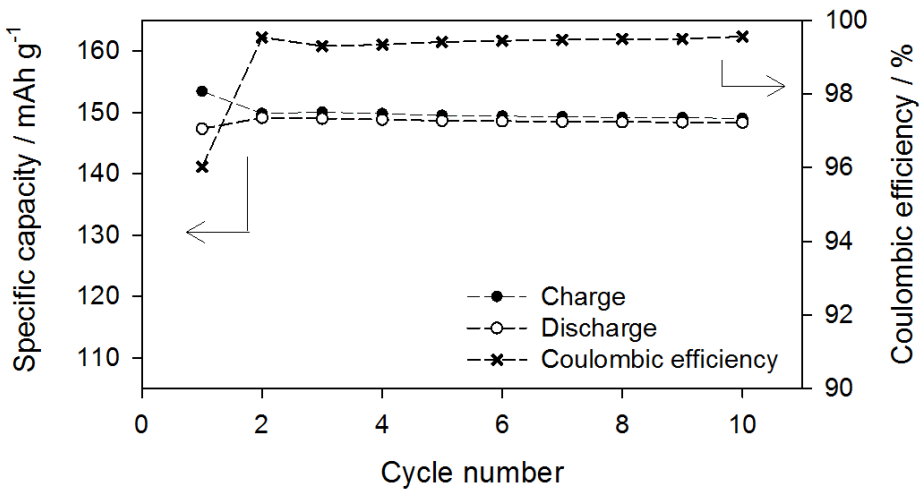

Figure 11 Coulombic efficiency and specific capacity of Li/LCO cell using fresh LCO and Li metal, and electrolyte solution collected after 70 ° C storage

4.1.3 Unraveling the degradation mechanism of surface films

In order to unravel the degradation mechanisms of surface films, their chemical compositions before and after 70 ° C storage were compared based on the XPS data. As shown in Fig. 12, their chemical composition changed notably after storage at 70 ° C. Most prominently, the peak for LiF (685 eV in F 1s) increased while those of C 1s decreased (Figs. 12a and 12b). For LiF enrichment in the surface film, the only possible source of F is $LiPF_6$ in the electrolyte. Therefore, some F-containing chemical species derived from $LiPF_6$ are assumed to be responsible for the deterioration of surface films. The most likely suspect is hydrogen fluoride (HF). HF can be generated from several routes, as discussed in Introduction. Experimentally, the acid concentration in the electrolyte after storage at 70 ° C for 10 h was about 400 ppm, being more than 7 times larger than that in the fresh electrolyte (55 ppm). Hence, the probability of HF generation is very high during the 70 ° C storage for attacking the films on the LCO surface. To examine this possibility, the pre-cycled LCO electrode was stored in an EC/DEC solution containing 400 ppm added HF under the same aging condition (70 ° C for 10 h). The resultant XPS spectra (Fig. 12c) look very similar to those from the sample stored at 70 ° C without HF addition (Fig. 12b). Therefore, the HF attack is very likely.

Another reactive F−containing species that may be derived from $LiPF_6$ is PF_5. This gaseous Lewis acid is generated by thermal decomposition of $LiPF_6$ at > 60 ° C, and thus its attack on the surface films is also probable. To examine this possibility, a control experiment was performed. The pre−cycled LCO electrode with deposited surface film was put in contact with PF_5 gas generated by heating 0.02 g of $LiPF_6$. Note that this amount of $LiPF_6$ is meant to simulate the concentration of $LiPF_6$ in the electrolyte solution (1.3 *M*). The XPS spectra obtained from the electrode after PF_5 exposure (Fig. 12d) are very different to those shown in Fig. 12b, with a noticeable difference in the F 1s and P 2p spectra. The peak intensity for LiF (685 eV in F 1s) decreases while those for P−O (135 eV in P $2p_{3/2}$ and 532 eV in O 1s) or PF_xO_y (135 eV in P $2p_{3/2}$, 533.5 eV in O 1s, and 688 eV in F 1s [71, 72]) increase. (Very similar XPS data were obtained when using a larger amount of $LiPF_6$, and thus they are omitted here.) This signifies that the PF_5 attack cannot account for the surface film damage.

To ascertain the HF attack on the surface films, the concentration of $LiPF_6$ in the electrolyte solution, which is the HF source, was reduced down to 0.5 *M* in the same solvents, and the cell was tested using the same routine: pre−cycling at 25 ° C, storage at 70 ° C for 10 h, and re−cycling at 25 ° C. The obtained cycling data with 0.5 *M* $LiPF_6$ (Fig. 13a) show that the charging capacity after 70 ° C storage

is much smaller than that observed with 1.3 *M* $LiPF_6$ (Fig. 7c). Consequently, the Coulombic efficiency in the first cycle of re-cycling is much larger than the case of 1.3 *M* (Fig. 7d). Fig. 13b compares the OCV drops traced during the 70 ° C storage for the two Li/LCO cells. Clearly, the retention time before the rapid OCV drop is extended for the cell with 0.5 *M* $LiPF_6$. This reflects that the reduction of LCO is retarded as the electrolyte oxidation is less serious, which in turn indicates that the retarded film damage is due to the suppressed HF generation with a lower $LiPF_6$ concentration in the electrolyte.

The reason for the poorer passivating ability of the damaged surface film was revealed by comparing the chemical compositions of surface films calculated from the XPS data before and after the storage. From Fig. 14, the atomic ratios of the damaged surface film (with 1.3 *M* $LiPF_6$/EC/DEC and stored at 70 ° C) are quite different from that of the undamaged one (i.e. before storage): the Li and F species are enriched while the C species are depleted during the 70 ° C storage. The enrichment of Li and F species in the damaged surface films can be accounted for by the HF attack. That is, for example, HF can attack lithium alkyl carbonates (LiOCOOR) and Li_2CO_3 inside surface film to generate LiF ($\mathbf{Li_2CO_3 + HF \rightarrow LiF + H_2CO_3, LiOCOOR + HF \rightarrow LiF + HOCOOR}$) among complex mixture of several chemical species of surface film which might react with HF.

The depletion of C species illustrates that the C-containing surface film components (which must be derived from the solvent molecules) are attacked by HF and removed from the films. The TEM images (Figs. 15a and 15b) illustrate that the damaged surface film is also much thinner. Furthermore, the surface film obtained in the HF contact experiment (70 ° C, added HF in EC/DEC) has a chemical composition quite similar to that of the damaged one (70 ° C, $LiPF_6$ in EC/DEC), supporting the HF attack on the surface film. The film thickness shown in Fig. 15c also suggests that HF attacks and etches the surface film.

Additionally, in SEM images, surface of LCO particle before storage (Figs. 16a and c) is smooth. After storage at 70 °C for 10 h (Figs. 16c and d), nano-sized grains were observed on the surface on the LCO. It can be inferred LiF particles which was observed in XPS results. This result is similar to the report suggested that LiF forms macroscopic cluster on $LiCoO_2$ surface [73]. It can be concluded that the uniformly covered organic surface film is attacked by HF and thinned, and the surface is non-uniformly covered with LiF.

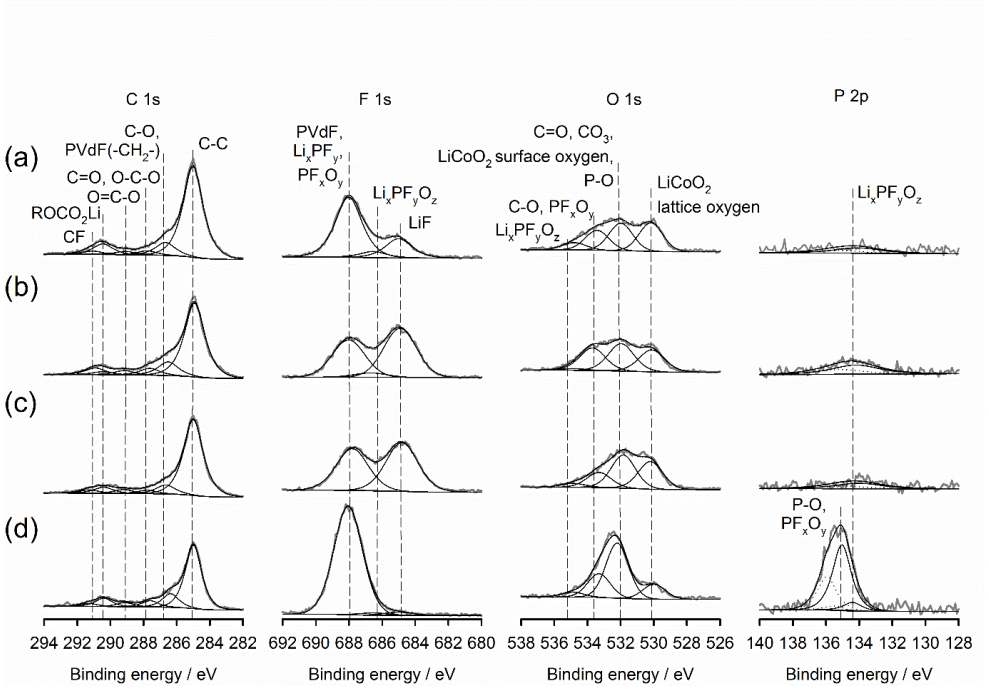

Figure 12 XPS spectra obtained from $LiCoO_2$ electrode surface (a) before storage (pre-cycled), (b) after storage at 70 ° C for 10 h in the standard electrolyte (1.3 *M* $LiPF_6$ in EC/DEC), (c) after storage at 70 ° C for 10 h in EC/DEC with 400 ppm added HF, and (d) after exposure to PF_5(g) for 10 h.

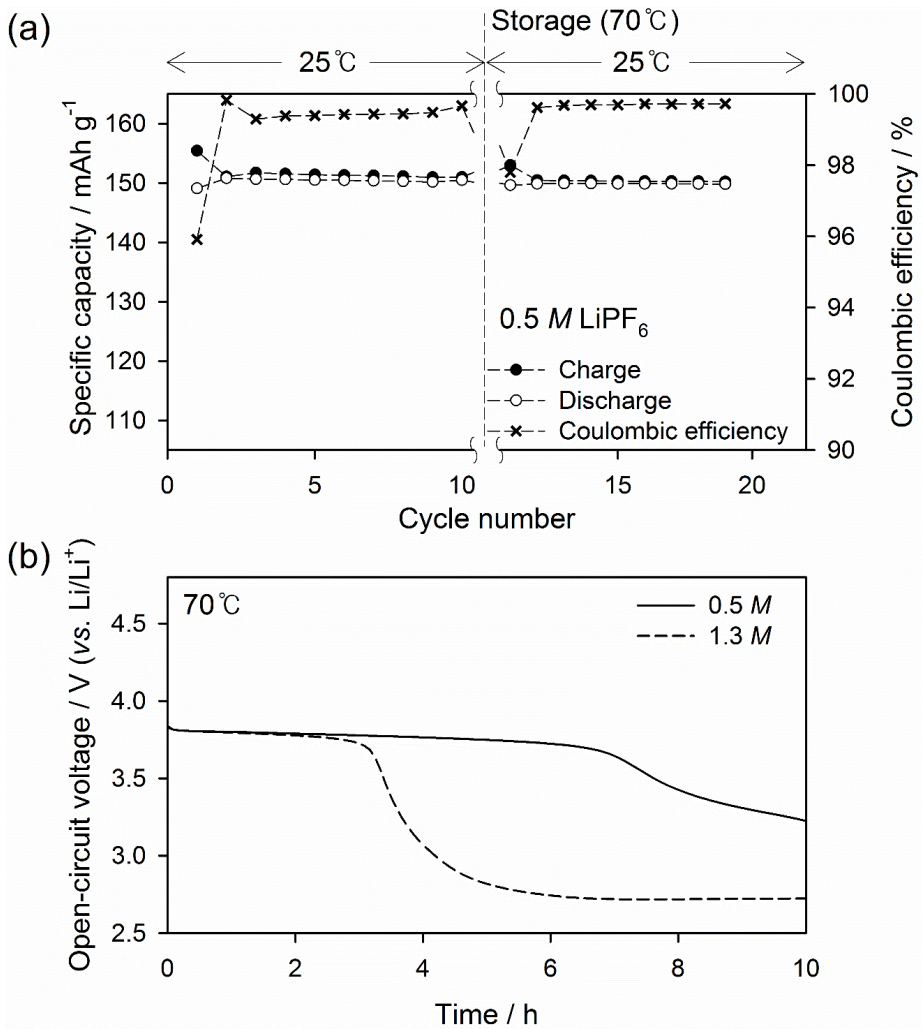

Figure 13 . (a) Variations of charge/discharge specific capacity and Coulombic efficiency of Li/$LiCoO_2$ cells before and after 70 ° C storage. The electrolyte was 0.5 *M* $LiPF_6$ in EC/DEC (3/7, v/v), and other experimental conditions were the same as for Fig. 7c. (b) Comparison of OCV decay for the two Li/LCO cells (with 0.5 and 1.3 *M* $LiPF_6$ in the electrolyte) traced during 70 ° C storage.

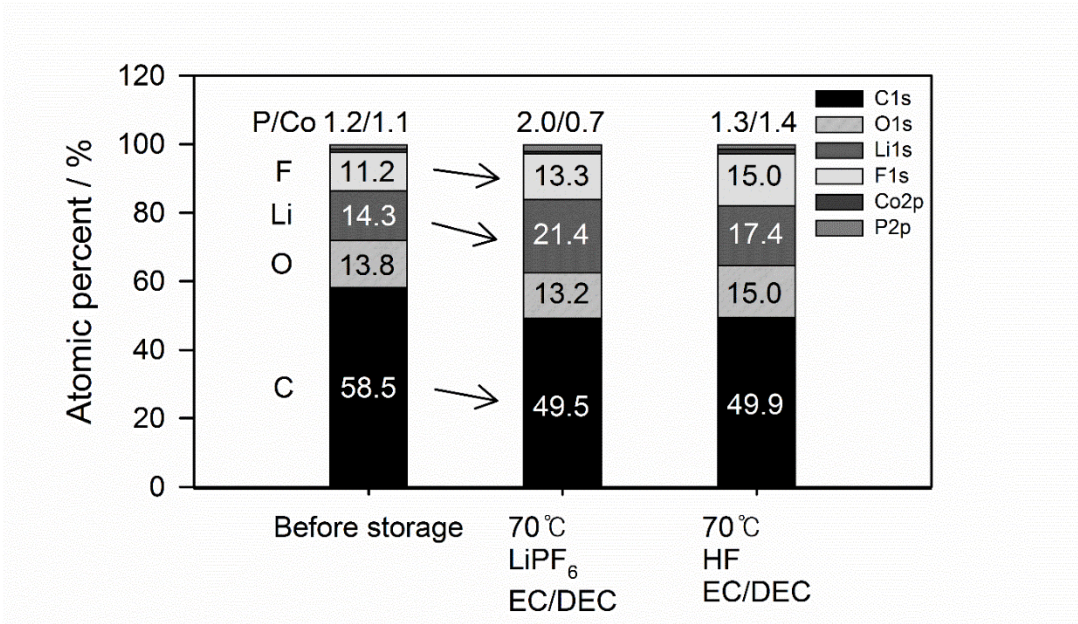

Figure 14 Atomic percentages of the elements in the surface films derived from XPS spectra. Three samples were compared: pre-cycled LCO electrode (before storage), after 70 ° C storage in the standard electrolyte, and after 70 ° C storage in EC/DEC with 400 ppm added HF.

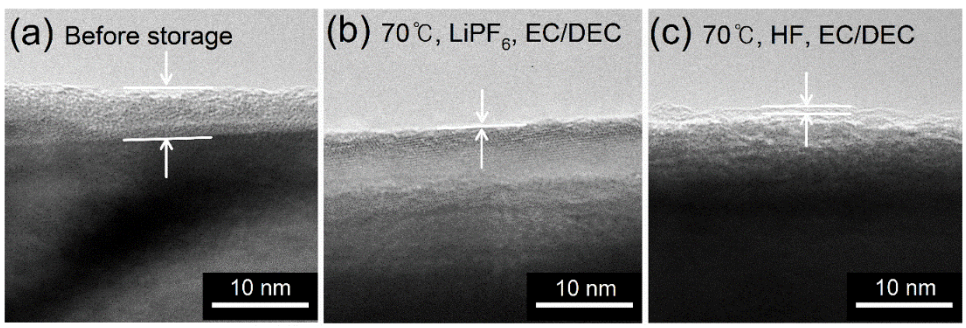

Figure 15 TEM images of (a) pre-cycled LCO, (b) after 70 ° C storage in the standard electrolyte, and (c) after 70 ° C storage in EC/DEC with 400 ppm added HF.

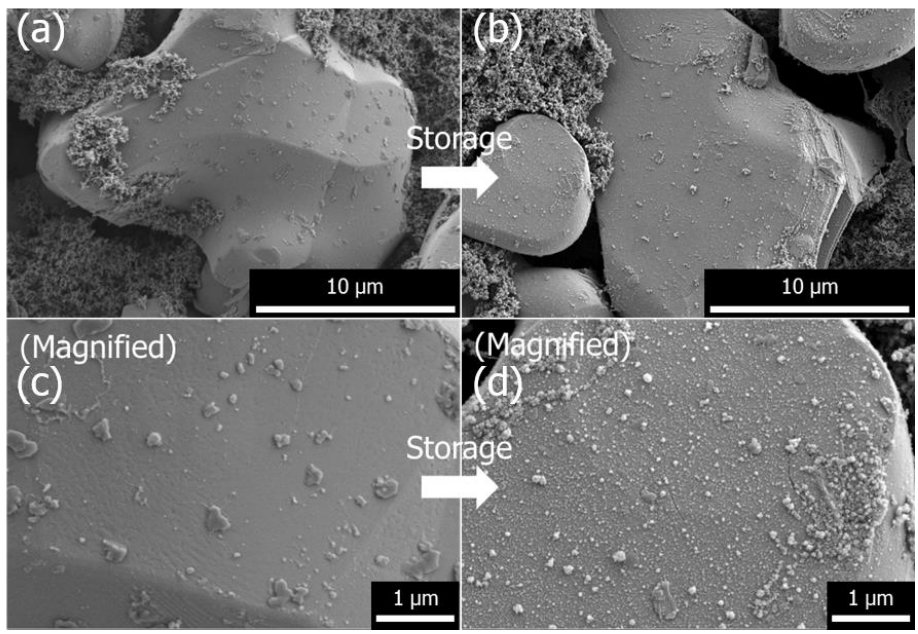

Figure 16 SEM images of the LCO electrodes (a) before and (b) after storage at 70 ° C in the standard electrolyte. (c) and (d) are magnified images of (a) and (b).

4.2 Behavior of surface film at higher State-Of-Charge (SOC) at moderately elevated temperature and its effect on cell performance

4.2.1 Degradation and repairing of surface films at moderately elevated temperature at its effect on cell performance

After 10 cycles of pre-cycling, the Li/LCO cells were set at SOC5, 10, 25, and 50 and stored at 70 °C. In Fig. 17, open-circuit voltages (OCVs) of the cells dropped to ca. 2.8 V (*vs.* Li/Li^+) (i.e. fully discharged). OCV drop means Li^+/e insertion into a vacant Li site of LCO and LCO is reduced. As discussed in above part 4.1, during storage at 70 °C, surface films on the LCO electrode degrades and loses its passivating ability. Electrolyte is oxidized on the naked LCO surface and Li^+/e insert into the LCO reducing LCO. In this process, surface films would be repaired by electrolyte oxidation. Degradation/repairing of surface films are continued until SOC of the cell reaches zero (i.e. Li^+/e site in LCO fully filled). In Fig. 17, the time that it takes to drop to be fully discharged (2.8 V (*vs.* Li/Li^+)) is approximately proportional to the SOC of the cell. Since the LCO electrode with higher SOC has larger amount of vacant Li^+/e site, it

takes longer to reach SOC0, and larger amount of electrolyte is oxidized.

To investigate whether the supposed surface film behavior (degradation/repairing) at high temperature affects the cell performance, after storage at 70 °C for 10 h, the cells were discharged and re-cycled (charge/discharge) at 25 °C. First of all, 'self-discharged capacity' during storage at 70 °C for 10 h was checked. As shown in Fig. 18, self-discharged capacity is the difference between charge capacity before storage (for SOC setting at 25 °C, for example, ca. 75 mA h g^{-1} for SOC 50 cell) and discharge capacity after storage (measured at 25 °C). Self-discharged capacity increases as SOC increases, and it was 21 mA h g^{-1} for the SOC50 cell (Table 1).

Secondly, the cells are divided into two groups based on the SOCs of the cells after storage for 10 h. One group is composed of SOC0, 5, and 10 cells (marked with red box in Fig. 17). They are almost discharged state (OCVs are ca. 2.8 V ~ 3.5 V (*vs.* Li/Li^+)). The surface films of LCO electrode of them are expected to be degraded. When LCO is fully discharged, surface films are attacked by HF at 70 °C (as discussed in part 4.1,) while electrolyte is not oxidized on LCO surface (because Li^+/e site of LCO is fully filled and LCO cannot be reduced). The other group is composed of SOC25 and 50 cells (marked with blue box in Fig. 17). After 10 h storage, their SOCs

exceed zero (OCVs are over 3.8 V (*vs.* Li/Li^+)). Since Li^+/e site in the LCO are not fully filled, surface film repairing (due to electrolyte oxidation) occurs for entire storage time, 10 h.

Fig. 19 shows Coulombic efficiencies of the five cells. In the first cycle of recycling (the 11^{th} cycle in total), Coulombic efficiencies of the first group (the cells of SOC0, 5, and 10 marked with red box) are about 92~95 %. It is much smaller than those of before storage cycles (ca. 98 %). On the other hand, Coulombic efficiencies of the second group (the cells of SOC25 and 50 marked with blue box) are about 98%, which are almost similar to those before storage.

To investigate what happens in the cells at the first cycle of recycling, charge/discharge capacities of the SOC0 and SOC50 cells were compared as the representative samples of two groups (Fig. 20, data of the SOC0 cell is the same as in Fig. 7c). While the SOC0 cell shows extra charge capacity after storage (as discussed in Part 4.1), the SOC50 cell shows similar charge/discharge capacity as before storage. In voltage profiles of the cells (Fig. 21), the SOC0 cell shows an additional charge capacity after storage in the voltage range over 4 V (*vs.* Li/Li^+) than before storage. It is extra charge capacity due to electrolyte oxidation. However, the SOC50 cell has similar voltage profiles before and after storage. That is, after storage, electrolyte oxidation does not increase compared to before storage. When a cell is stored at higher SOC, and SOC exceeds zero at the end of storage,

after storage, the LCO electrode is passivated by repaired surface films, and electrolyte oxidation is suppressed on it.

For the SOC50 cell, the self-discharged capacity during storage at 70 °C for 10 h is ca. 21 mA h g^{-1} (Table 1). Suppressed extra charge capacity due to passivating ability of repaired surface film is ca. 10 mA h g^{-1} comparing that of the SOC0 cell (Fig. 20). The cell of higher SOC suffers from capacity loss by self-discharge (due to degradation and repairing of surface film) during storage at high temperature, while charge capacity after storage does not increase (and Coulombic efficiency does not decrease) compared to before storage, due to repaired surface film. It is different with the result of the SOC0 cell where extra charge capacity increases after storage. Degradation behaviors of Li/LCO cells at high temperature are somewhat different depending on the SOC of the cell and the state of surface films (degraded or repaired) at the end of storage.

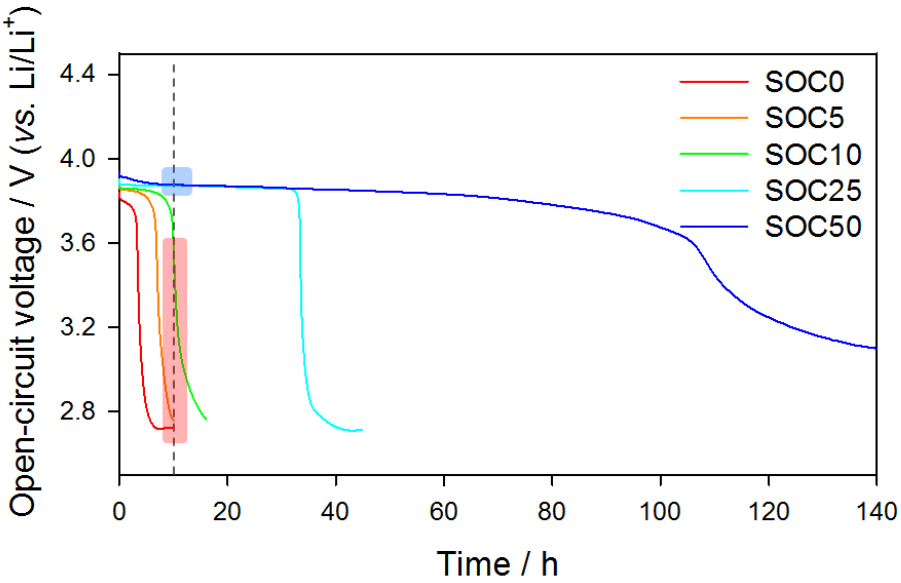

Figure 17 OCV profiles of Li/LCO cells of various SOCs during storage at 70 °C. After 10 h of storage, they are divided into two groups by remaining SOC (Red and blue box each).

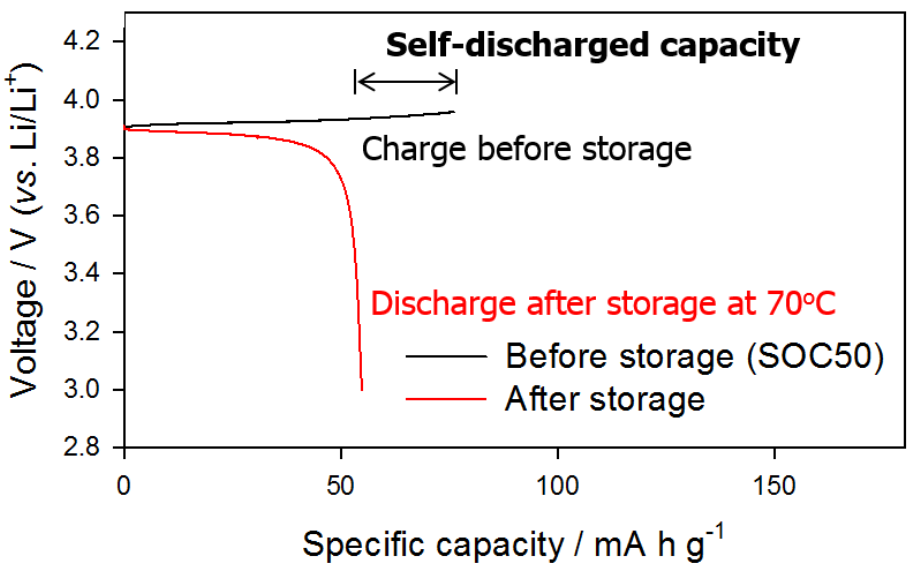

Figure 18 The graph illustrating how to measure self-discharged capacity during storage

SOC	Self-discharged capacity [mA h g^{-1}]
0	~ 0
5	7
10	15
25	20
50	21

Table 1 Self-discharged capacities of the cells during storage at 70 °C for 10 h

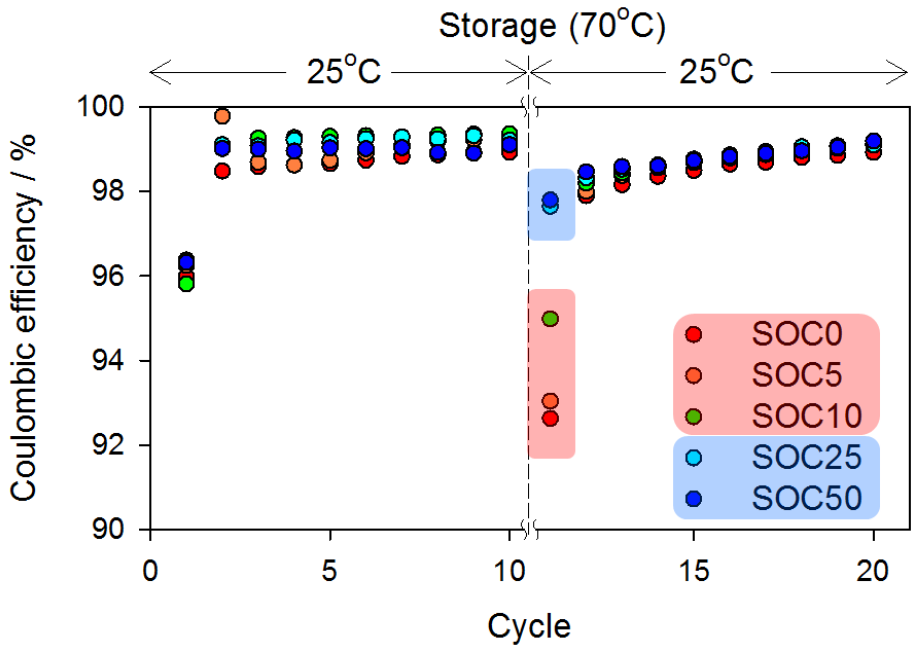

Figure 19 Coulombic efficiencies of the cells before and after storage at 70°C for 10 h

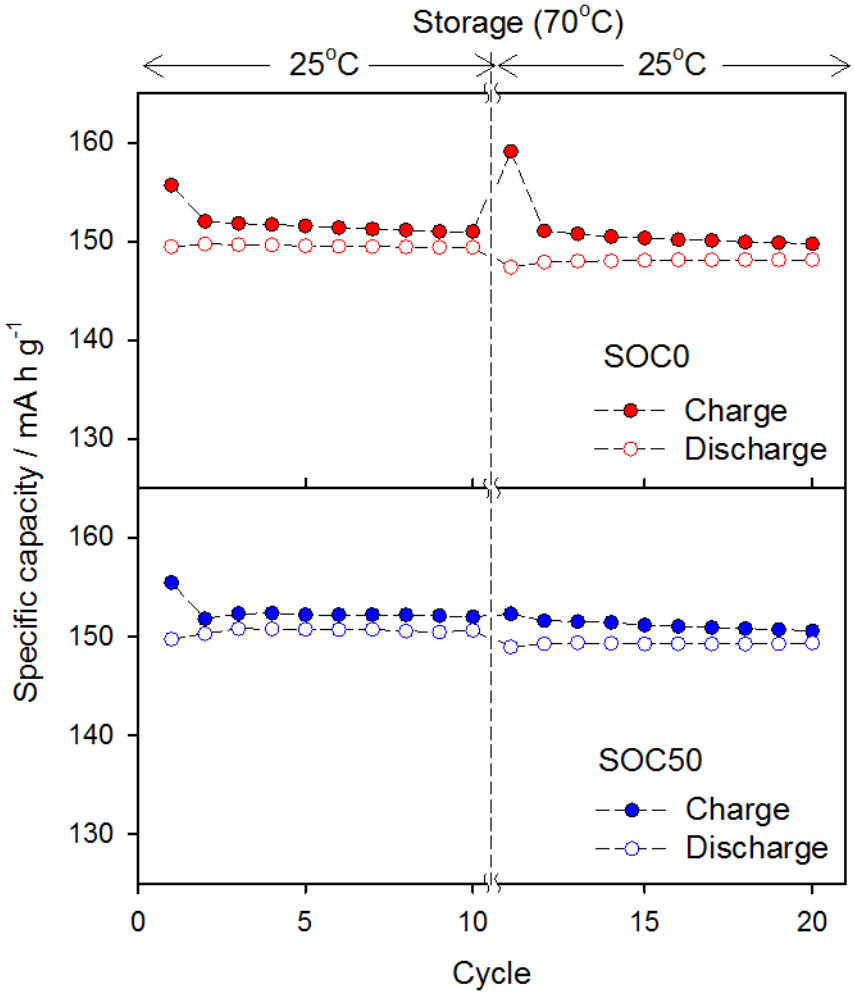

Figure 20 Charge and discharge capacities of the SOC0 cell and the SOC50 cell (data of the SOC0 cell is the same as Fig. 7c).

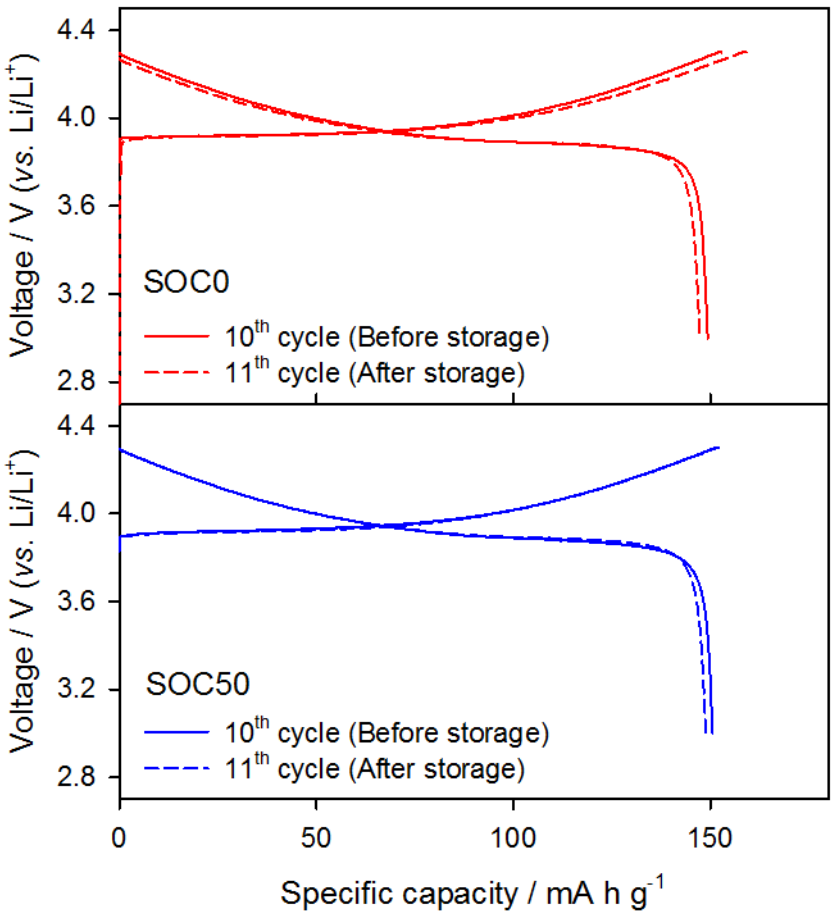

Figure 21 Voltage profiles of the SOC0 cell and the SOC50 cell before and after storage

4.2.2 Identification of repaired surface films using spectroscopic experiments

To check the above scenario of surface film repairing is plausible, some spectroscopic analyses were conducted. XPS analysis was conducted (Fig. 22) for electrode of SOC50 cell. Before storage (after pre-cycling), organic and inorganic materials which are known to surface films are detected. There are peaks of C=O and CO_3 (532 eV), and C-O (533.5 eV) in the O 1s spectra as well as LCO lattice oxygen (530 eV). In C 1s spectra, there are peaks of C-C, C-H (285 eV), C-O (286.5 eV), C=O (287.8 eV), O-C=O (289.0 eV), CO_3 (290.6 eV) and CF_x (291.6 eV). In F 1s, LiF (685 eV) and $Li_xPF_yO_z$ (686.5 eV) are detected. They are similar with those of SOC0 electrode before storage (Fig. 12a). Similar to the results in Part 4.1, organic materials generated by electrolyte oxidation, and salt byproducts cover the LCO. After storage at 70 ° C for 10 h, the peaks including F 1s, O 1s and C 1s are similar to those before storage. The surface film, composed of materials similar to those before storage, is repaired during high temperature storage, due to electrolyte oxidation on degraded LCO surface by HF attack. In the atomic ratio (Fig. 23), the proportions of lithium, fluorine, carbon and oxygen are similar to those before storage.

In the SEM images (Figs. 24a and b), the electrode surfaces of SOC50 cell before and after the storage look smooth and similar to each other. In the TEM images (Figs. 24c and d), the films are uniform and have a thickness of about 5 nm before and after storage. In summary, the repaired surface films are uniformly covered, and have similar compositions, shape, and passivating ability to those of the films before storage.

Compared to the degraded surface films of the SOC0 cell (Part 4.1) which are thin, non-uniform and non-passivate, the repaired surface films uniformly cover LCO surface and passivate the LCO surface.

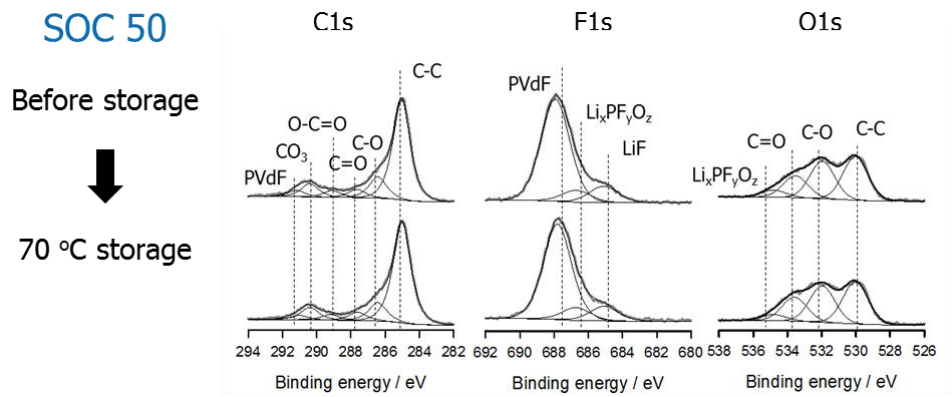

Figure 22 XPS spectra of surface films on LCO electrodes at SOC50 before and after storage at 70 °C

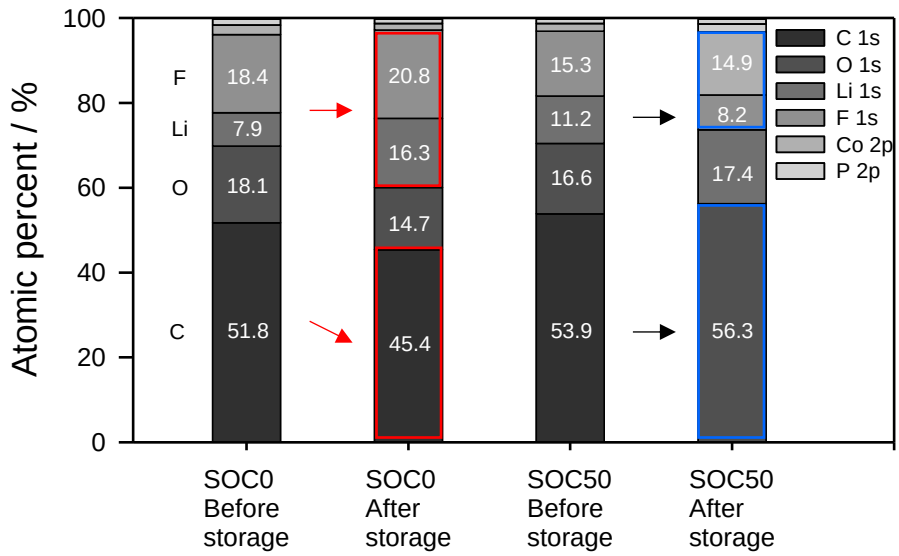

Figure 23 Atomic ratio of the LCO electrodes calculated from XPS result. Before and after storage at 70 ℃ of the SOC0 cell and the SOC50 cell

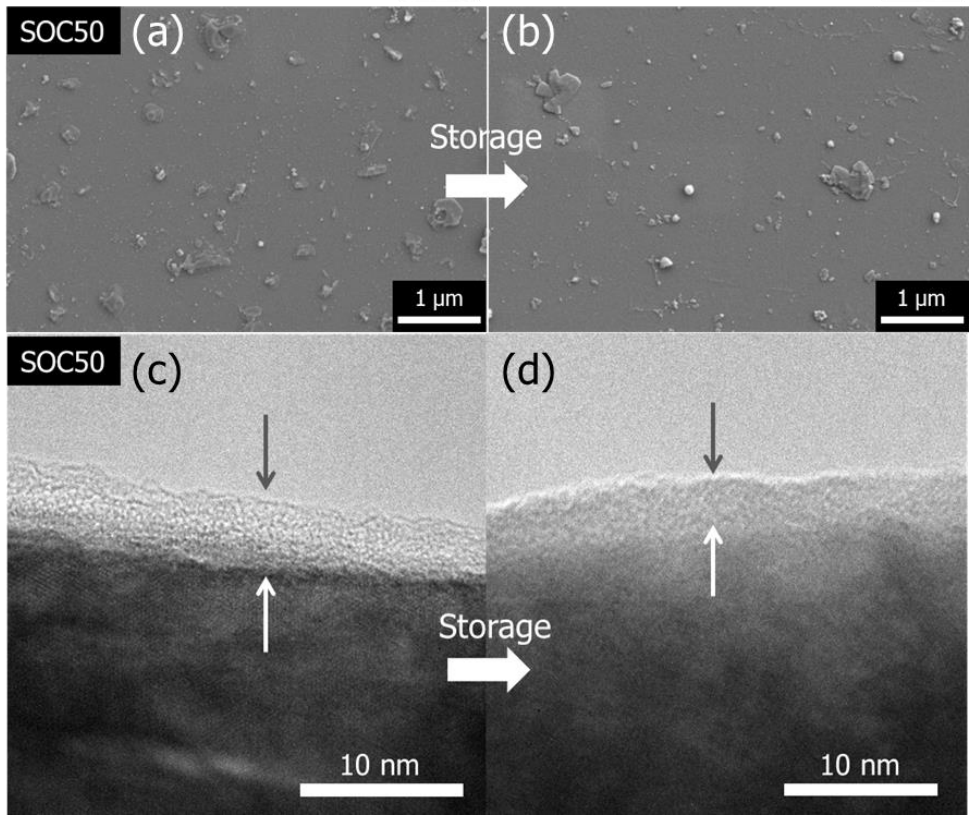

Figure 24 SEM images of LCO electrodes of the SOC50 cell (a) before and (b) after storage at 70 °C. TEM images of surface films on LCO electrodes of the SOC50 cell (c) before and (d) after storage at 70 °C.

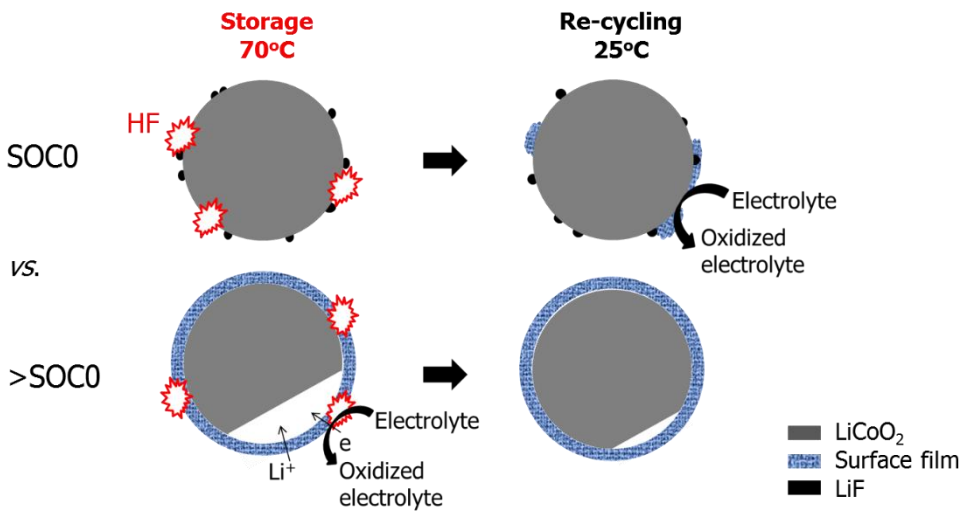

Figure 25 Schematic illustration of surface film behaviors of the electrodes of the two groups and effects on the cells during and after storage

4.2.3 Effect on the degradation of the full-cell

Surface films of negative electrodes such as graphite or silicon are degraded at moderately elevated temperature [29, 74] like surface films of LCO electrode. When graphite/LCO full-cell is exposed to moderately elevated temperature, the cell can be degraded because of surface film degradations both of negative and positive electrode. To predict the degradation of full-cell, for simplicity, it is assumed that surface films of negative electrode are not degraded. When the cell is stored at somewhat charged state (like the second group of part 4.2.1, Fig. 26), LCO is self-discharged and Li^+/e is inserted into LCO during storage at 70 °C and the cell loses charged energy. When LCO is stored at SOC0 (or low SOC, like the first group of part 4.2.1, Fig. 27), after storage, extra charge capacity is consumed because of electrolyte oxidation. Both cases make cell' s capacities degraded. Unbalance between negative and positive electrode (N/P ratio), and Li^+ loss of the cell shorten cell life.

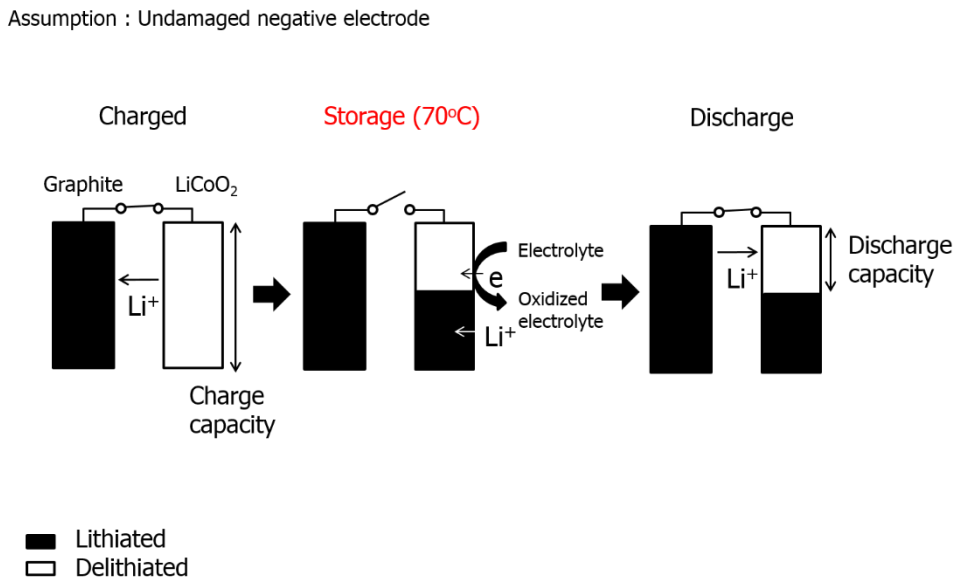

Figure 26 Schematic diagram of capacity loss of full-cell during storage at 70 °C, when LCO electrode is charged before storage

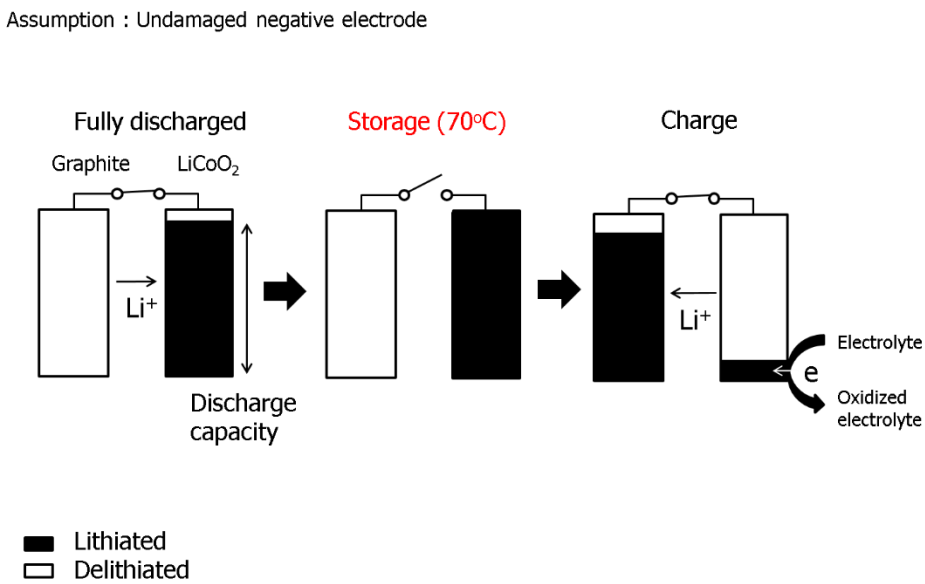

Figure 27 Schematic diagram of capacity loss of full-cell during and after storage at 70 °C, when LCO electrode is discharged before storage.

4.3 A countermeasure to mitigate cell degradation at moderately elevated temperature: HF scavenger (cupper(II) oxide, CuO) addition into LCO electrode to suppress surface film degradation

4.3.1 Effect of CuO on surface film degradation and cell performance degradation

First of all, to investigate whether CuO removes HF, the CuO-containing electrolyte was stored at 70 °C. There was ca. 20 ppm of HF in the fresh electrolyte. After storage at 70 °C for 6 h, HF concentration in the CuO-containing electrolyte was 80 ppm whereas it was 140 ppm in the CuO-free electrolyte. CuO removes HF, produced in the electrolyte at 70 °C ($CuO+HF \rightarrow CuF_x \cdot H_2O$ [36]).

In Fig. 28, open-circuit voltages (OCVs) of the cells during storage at 70 °C are graphed. OCV decrease of the cell means electrons and lithium ions are co-injected into vacant Li site of $Li_{1-x}CoO_2$ as we discussed in above part 4.1. In this process, the surface film of the pre-cycled LCO electrode deteriorates and the passivation ability deteriorates, resulting in the influx of Li^+/e into the electrode with electrolyte oxidation. During storage at 70 °C, OCV of the CuO-added

cell decreases more slowly than that of CuO-free cell. After 6 h of storage, OCV of the CuO-added cell is about 3.7 V (*vs.* Li/Li^+) and OCV of the CuO-free cell is about 2.8 V (*vs.* Li/Li^+). It could be supposed that added CuO in LCO electrode helps the surface degradation delayed. So passivation ability degradation is mitigated.

To investigate its effect on cell performance, cycle performances were checked. In Fig. 29, at the first cycle of re-cycling after storage, charge capacity of the CuO-added cell is smaller than that of the CuO-free cell, and Coulombic efficiency of CuO-added cell is higher than that of the CuO-free cell. This means that electrolyte oxidation on the CuO-added LCO electrode, after storage, is suppressed than on the CuO-free LCO electrode, probably due to passivating ability of surface films on CuO-added LCO electrode, after storage. During storage at 70 °C, reactive HF, generated in the cell, is captured by CuO, and its attack on the surface films is suppressed. Sequentially, electrolyte oxidation on degraded LCO surface, and reduction of LCO are mitigated. At 6 h of storage time, surface films of CuO-added LCO electrode are repaired, due to still empty Li^+/e site of LCO, whereas surface films of CuO-free LCO electrode are degraded, because of completely filled Li^+/e site of LCO.

Self-discharged capacity of the CuO-added cell at SOC50 (Table 2, 7 mA h g^{-1}) during storage at 70 °C for 10 h, is smaller than that of the CuO-free cells (21 mA h g^{-1}, same as the data of Table 1).

CuO in the LCO electrode suppresses HF attack on surface films of LCO electrode, so that electrolyte oxidation accompanying self-discharge of LCO is alleviated. Degradations of both discharged or charged state cells are mitigated by addition of the HF scavenger, and mitigation of surface film degradation.

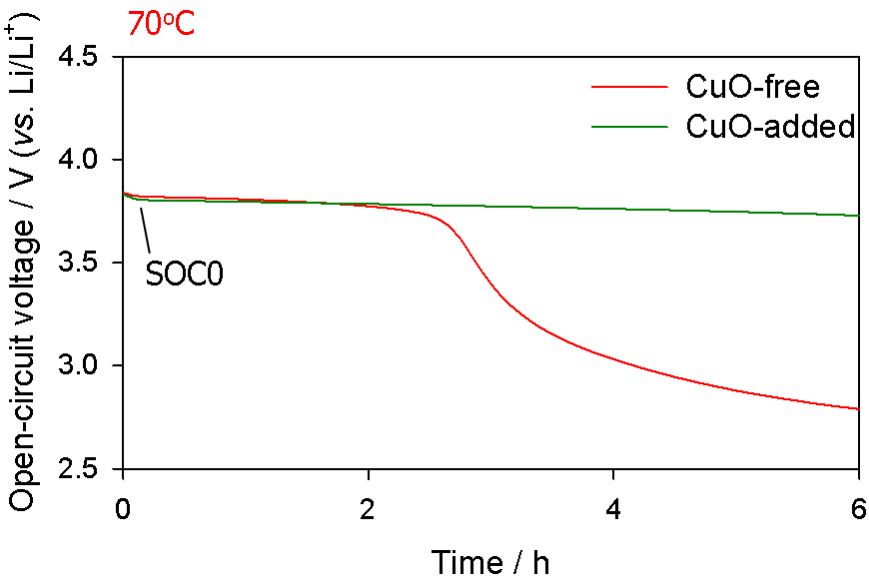

Figure 28 OCV plots of CuO-free and CuO-added Li/LCO cell during storage at 70 °C (Data of the CuO-free cell is same as the data of Fig.8)

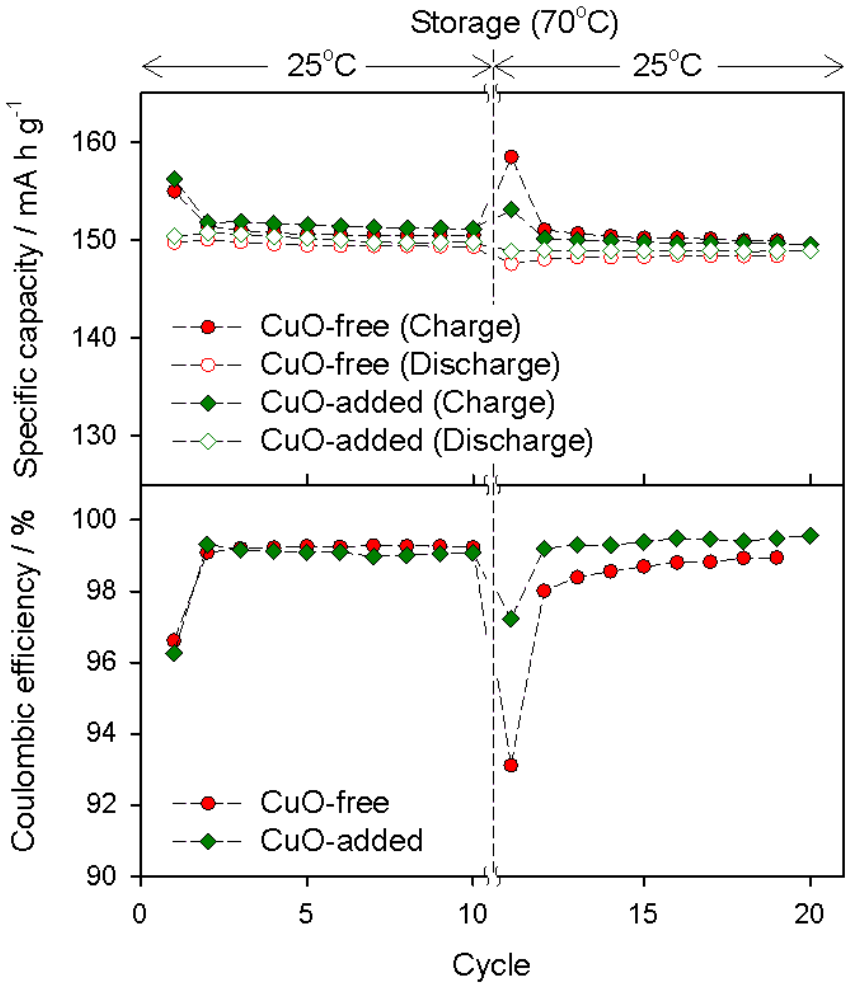

Figure 29 Charge and discharge capacities and Coulombic efficiencies of CuO-free and CuO-added cells. They are stored at 70 °C for 6 h after 10 cycles of pre-cycling.

	Self-discharged capacity during storage [mA h g^{-1}]	
	CuO-free	**CuO-added**
SOC0	< 4	< 4
SOC50	21	7

Table 2 Self-discharged capacities of CuO-free and CuO-added Li/LCO cells during storage at 70 °C for 10 h. (Data of CuO-free cell is the same as the data of Table 1)

4.3.2 Spectroscopic analysis of surface films on CuO-added LCO electrode

Using spectroscopic experiments, surface films of CuO-added LCO electrode before and after storage at 70 °C for 6 h were investigated. Through XPS results (Fig. 30), the spectra of elements of surface films represented by C 1s, O 1s, and F 1s are similar before and after storage at 70 °C.

In SEM images (Fig. 31 (a) and (b)), both before and after storage, the LCO surfaces are smooth and clean, and have some hundreds of nanometers of particles dispersed, presumably suspected as CuO (Cu was detected on these particles using Energy Dispersive X-ray Spectroscopy (EDS) of the SEM instrument). In TEM images (Fig. 31 (c) and (d)), there are similar surface films on LCO particles before and after storage with ca. 5 nm thickness. For CuO-added LCO electrode, surface films are preserved after storage at 70 °C for 6 h, as discussed above.

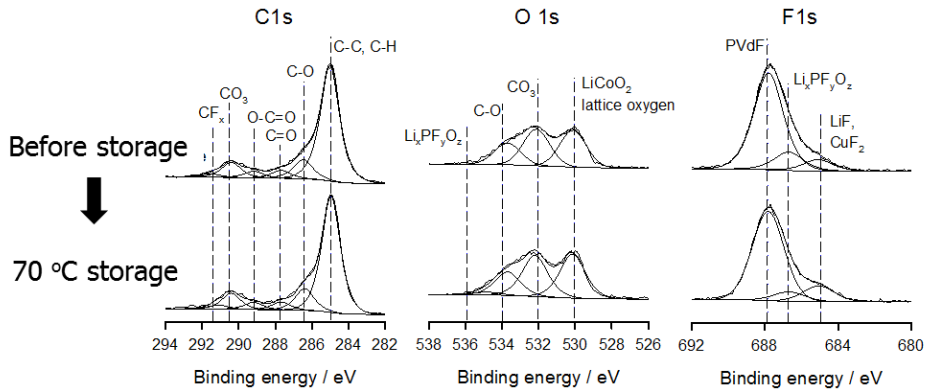

Figure 30 C 1s, O 1s and F 1s XPS spectra of CuO-added LCO electrode before and after storage at 70 °C

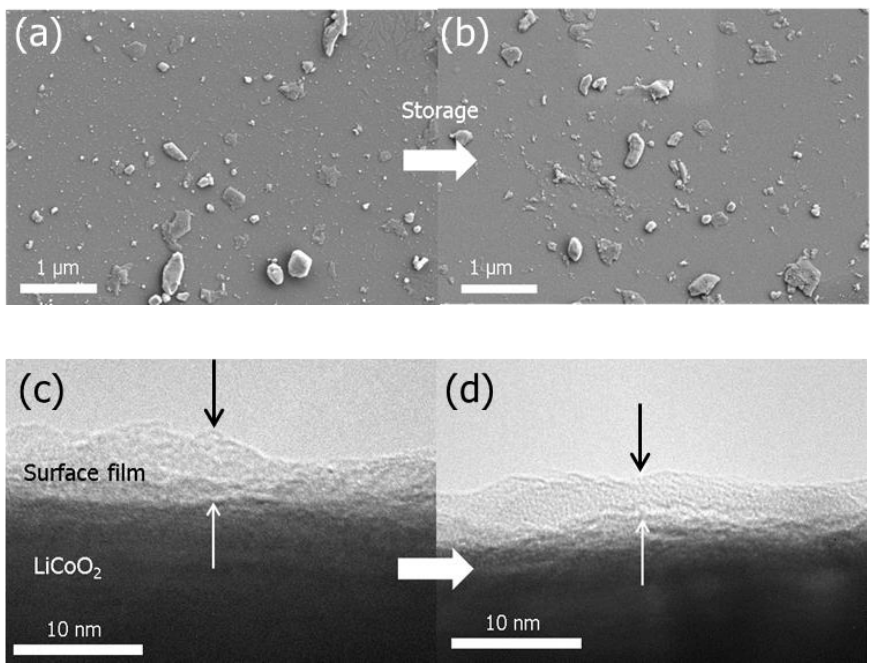

Figure 31 SEM images of CuO-added LCO electrode (a) before and (b) after storage at 70 °C. TEM images of surface films on CuO-added LCO electrode (c) before and (d) after storage at 70 °C

5 Conclusion

In this study, degradation of the surface film on $LiCoO_2$ (LCO) at moderately elevated temperature, its effects on cell performance, and appropriate countermeasure were studied. The major findings are summarized below.

In the first part, we designed experiments to examine degradation the surface films on LCO at moderately elevated temperature. (i) The surface film on the LCO electrode generated during pre-cycling is damaged upon storage at 70 ° C for 10 h. The postmortem analyses indicate that the surface film becomes thinner and its chemical composition changes: inorganic species such as LiF are enriched at the expense of the C-containing organic species. (ii) The surface film is degraded by attack of HF generated from $LiPF_6$ during the storage. (iii) After the thermal storage, the Li/LCO cell shows extra charging capacity to cause a poorer Coulombic efficiency, due to electrolyte oxidation on the damaged LCO surface.

In the second part, when the cell is exposed to elevated temperature at higher State-Of-Charge (SOC), (i) surface films are repaired due to electrolyte oxidation on the damaged LCO surface during storage at elevated temperature. Composition, feature and

passivating ability of repaired films are similar with those of before storage. (ii) The cell suffers from capacity loss by self-discharge during storage because of surface film degradation/repairing. However, it does not suffer from extra charge capacity, after storage. It shows similar charge capacity and Coulombic efficiency to before storage, due to repaired surface film.

In the third part, the degradation of the cell is mitigated by addition of HF scavenger, CuO. (i) When CuO is added into LCO electrode, surface film degradation is delayed at moderately elevated temperature. (ii) Due to mitigated degradation of surface films, when the CuO-added cell is stored at lower SOC, the cell shows smaller extra charge capacity after 70 °C storage, than CuO-free cell. It is merit on electrolyte oxidation and Coulombic efficiency of the cell. When the CuO-added cell is stored at 70 °C at higher SOC, self-discharged capacity decreases during exposure to high temperature, than that of CuO-free cell.

References

[1] H. Maleki, G. Deng, A. Anani, J. Howard, Thermal Stability Studies of Li-Ion Cells and Components, Journal of The Electrochemical Society, 146 (1999) 3224-3229.

[2] S. Watanabe, M. Kinoshita, K. Nakura, Capacity fade of $LiNi_{(1-x-y)}Co_xAl_yO_2$ cathode for lithium-ion batteries during accelerated calendar and cycle life test. I. Comparison analysis between $LiNi_{(1-x-y)}Co_xAl_yO_2$ and $LiCoO_2$ cathodes in cylindrical lithium-ion cells during long term storage test, Journal of Power Sources, 247 (2014) 412-422.

[3] T.M. Bandhauer, S. Garimella, T.F. Fuller, A Critical Review of Thermal Issues in Lithium-Ion Batteries, Journal of The Electrochemical Society, 158 (2011) R1-R25.

[4] J. Vetter, P. Novák, M.R. Wagner, C. Veit, K.C. Möller, J.O. Besenhard, M. Winter, M. Wohlfahrt-Mehrens, C. Vogler, A. Hammouche, Ageing mechanisms in lithium-ion batteries, Journal of Power Sources, 147 (2005) 269-281.

[5] Y. Shigematsu, S.-i. Kinoshita, M. Ue, Thermal Behavior of a C / $LiCoO_2$ Cell, Its Components, and Their Combinations and the Effects of Electrolyte Additives, Journal of The Electrochemical Society, 153 (2006) A2166-A2170.

[6] H. Tsunekawa, a. Tanimoto, Satoshi, R. Marubayashi, M. Fujita, K. Kifune, M. Sano, Capacity Fading of Graphite Electrodes Due to the Deposition of Manganese Ions on Them in Li-Ion Batteries, Journal of The Electrochemical Society, 149 (2002) A1326-A1331.

[7] S. Komaba, N. Kumagai, Y. Kataoka, Influence of manganese(II), cobalt(II), and nickel(II) additives in electrolyte on performance of graphite anode for lithium-ion batteries, Electrochimica Acta, 47 (2002) 1229-1239.

[8] H. Nara, K. Morita, T. Yokoshima, D. Mukoyama, T. Momma, T. Osaka, Electrochemical impedance spectroscopy analysis with a symmetric cell for $LiCoO_2$ cathode degradation correlated with Co dissolution, AIMS Materials Science, 3 (2016) 448-459.

[9] X. Zhang, B. Winget, M. Doeff, J.W. Evans, T.M. Devine, Corrosion of Aluminum Current Collectors in Lithium-Ion Batteries with Electrolytes Containing $LiPF_6$, Journal of The Electrochemical Society, 152 (2005) B448-B454.

[10] K. Xu, Nonaqueous liquid electrolytes for lithium-based rechargeable batteries, Chemical reviews, 104 (2004) 4303-4418.

[11] A. Veluchamy, C.-H. Doh, D.-H. Kim, J.-H. Lee, H.-M. Shin, B.-S. Jin, H.-S. Kim, S.-I. Moon, Thermal analysis of Li_xCoO_2 cathode material of lithium ion battery, Journal of Power Sources, 189 (2009) 855-858.

[12] A.V. Plakhotnyk, L. Ernst, R. Schmutzler, Hydrolysis in the system $LiPF_6$—propylene carbonate—dimethyl carbonate—H_2O, Journal of Fluorine Chemistry, 126 (2005) 27−31.

[13] S.E. Sloop, J.K. Pugh, S. Wang, J.B. Kerr, K. Kinoshita, Chemical Reactivity of PF_5 and $LiPF_6$ in Ethylene Carbonate/Dimethyl Carbonate Solutions, Electrochemical and Solid−State Letters, 4 (2001) A42−A44.

[14] V. Kraft, M. Grützke, W. Weber, M. Winter, S. Nowak, Ion chromatography electrospray ionization mass spectrometry method development and investigation of lithium hexafluorophosphate−based organic electrolytes and their thermal decomposition products, Journal of Chromatography A, 1354 (2014) 92−100.

[15] S. Wilken, M. Treskow, J. Scheers, P. Johansson, P. Jacobsson, Initial stages of thermal decomposition of $LiPF_6$−based lithium ion battery electrolytes by detailed Raman and NMR spectroscopy, RSC Advances, 3 (2013) 16359−16364.

[16] R. Yazami, A. Martinent, Chapter 8 − Fluorinated anions and electrode/electrolyte stability in lithium batteries A2 − Nakajima, Tsuyoshi, in: H. Groult (Ed.) Fluorinated Materials for Energy Conversion, Elsevier Science, Amsterdam, 2005, pp. 173−194.

[17] L. Terborg, S. Weber, F. Blaske, S. Passerini, M. Winter, U. Karst, S. Nowak, Investigation of thermal aging and hydrolysis

mechanisms in commercial lithium ion battery electrolyte, Journal of Power Sources, 242 (2013) 832-837.

[18] T. Kawamura, A. Kimura, M. Egashira, S. Okada, J.-I. Yamaki, Thermal stability of alkyl carbonate mixed-solvent electrolytes for lithium ion cells, Journal of Power Sources, 104 (2002) 260-264.

[19] M. Liu, F. Dai, Z. Ma, M. Ruthkosky, L. Yang, Improved electrolyte and its application in $LiNi_{1/3}Mn_{1/3}Co_{1/3}O_2$-Graphite full cells, Journal of Power Sources, 268 (2014) 37-44.

[20] S.F. Lux, J. Chevalier, I.T. Lucas, R. Kostecki, HF Formation in $LiPF_6$-Based Organic Carbonate Electrolytes, ECS Electrochemistry Letters, 2 (2013) A121-A123.

[21] L. Zheng, H. Zhang, P. Cheng, Q. Ma, J. Liu, J. Nie, W. Feng, Z. Zhou, $Li[(FSO_2)(n-C_4F_9SO_2)N]$ versus $LiPF_6$ for graphite/$LiCoO_2$ lithium-ion cells at both room and elevated temperatures: A comprehensive understanding with chemical, electrochemical and XPS analysis, Electrochimica Acta, 196 (2016) 169-188.

[22] D. Aurbach, K. Gamolsky, B. Markovsky, Y. Gofer, M. Schmidt, U. Heider, On the use of vinylene carbonate (VC) as an additive to electrolyte solutions for Li-ion batteries, Electrochimica Acta, 47 (2002) 1423-1439.

[23] E. Peled, S. Menkin, Review—SEI: Past, Present and Future, Journal of The Electrochemical Society, 164 (2017) A1703-A1719.

[24] N. Liu, H. Li, Z. Wang, X. Huang, L. Chen, Origin of Solid Electrolyte Interphase on Nanosized $LiCoO_2$, Electrochemical and Solid-State Letters, 9 (2006) A328-A331.

[25] T. Eriksson, A.M. Andersson, A.G. Bishop, C. Gejke, T. Gustafsson, J.O. Thomas, Surface Analysis of $LiMn_2O_4$ Electrodes in Carbonate-Based Electrolytes, Journal of The Electrochemical Society, 149 (2002) A69-A78.

[26] K. Xu, Electrolytes and Interphases in Li-Ion Batteries and Beyond, Chemical Reviews, 114 (2014) 11503-11618.

[27] A.M. Andersson, K. Edström, Chemical Composition and Morphology of the Elevated Temperature SEI on Graphite, Journal of The Electrochemical Society, 148 (2001) A1100-A1109.

[28] H. Park, T. Yoon, J. Mun, J.H. Ryu, J.J. Kim, S.M. Oh, A Comparative Study on Thermal Stability of Two Solid Electrolyte Interphase (SEI) Films on Graphite Negative Electrode, Journal of The Electrochemical Society, 160 (2013) A1539-A1543.

[29] J. Kim, J.G. Lee, H.-s. Kim, T.J. Lee, H. Park, J.H. Ryu, S.M. Oh, Thermal Degradation of Solid Electrolyte Interphase (SEI) Layers by Phosphorus Pentafluoride (PF_5) Attack, Journal of The Electrochemical Society, 164 (2017) A2418-A2425.

[30] D. Aurbach, B. Markovsky, G. Salitra, E. Markevich, Y. Talyossef, M. Koltypin, L. Nazar, B. Ellis, D. Kovacheva, Review on electrode-electrolyte solution interactions, related to cathode

materials for Li-ion batteries, Journal of Power Sources, 165 (2007) 491-499.

[31] A.M. Andersson, D.P. Abraham, R. Haasch, S. MacLaren, J. Liu, K. Amine, Surface Characterization of Electrodes from High Power Lithium-Ion Batteries, Journal of The Electrochemical Society, 149 (2002) A1358-A1369.

[32] K. Kim, D. Kam, C.C. Nguyen, S.W. Song, R. Kostecki, Study on the dominant film-forming site among components of $Li(Ni_{1/3}Co_{1/3}Mn_{1/3})O_2$ cathode in Li-ion batteries, Bulletin of the Korean Chemical Society, 32 (2011) 2571-2576.

[33] R. Dedryvère, H. Martinez, S. Leroy, D. Lemordant, F. Bonhomme, P. Biensan, D. Gonbeau, Surface film formation on electrodes in a $LiCoO_2$/graphite cell: A step by step XPS study, Journal of Power Sources, 174 (2007) 462-468.

[34] W.J. Lee, K. Prasanna, Y.N. Jo, K.J. Kim, H.S. Kim, C.W. Lee, Depth profile studies on nickel rich cathode material surfaces after cycling with an electrolyte containing vinylene carbonate at elevated temperature, Physical Chemistry Chemical Physics, 16 (2014) 17062-17071.

[35] D. Aurbach, Review of selected electrode-solution interactions which determine the performance of Li and Li ion batteries, Journal of Power Sources, 89 (2000) 206-218.

[36] J. Soon, T.J. Lee, H.-s. Kim, J. Jung, J.H. Ryu, S.M. Oh, Copper Oxide as a Hydrogen Fluoride Scavenger for High-Voltage $LiNi_{0.5}Mn_{1.5}O_4$ Positive Electrode, Journal of The Electrochemical Society, 164 (2017) A2677-A2682.

[37] 오승모, 전기화학(2 판), 자유아카데미 2014.

[38] T. Ohzuku, A. Ueda, Solid-State Redox Reactions of $LiCoO_2$ (R-3m) for 4 Volt Secondary Lithium Cells, Journal of The Electrochemical Society, 141 (1994) 2972-2977.

[39] T. Nohma, H. Kurokawa, M. Uehara, M. Takahashi, K. Nishio, T. Saito, Electrochemical characteristics of $LiNiO_2$ and $LiCoO_2$ as a positive material for lithium secondary batteries, Journal of Power Sources, 54 (1995) 522-524.

[40] S. Watanabe, M. Kinoshita, T. Hosokawa, K. Morigaki, K. Nakura, Capacity fade of $LiAl_yNi_{1-x-y}Co_xO_2$ cathode for lithium-ion batteries during accelerated calendar and cycle life tests (surface analysis of $LiAl_yNi_{1-x-y}Co_xO_2$ cathode after cycle tests in restricted depth of discharge ranges), Journal of Power Sources, 258 (2014) 210-217.

[41] S. Zheng, R. Huang, Y. Makimura, Y. Ukyo, C.A.J. Fisher, T. Hirayama, Y. Ikuhara, Microstructural Changes in $LiNi_{0.8}Co_{0.15}Al_{0.05}O_2$ Positive Electrode Material during the First Cycle, Journal of The Electrochemical Society, 158 (2011) A357.

[42] X. Lou, X. Zhao, X. He, Boron doping effects in electrochromic properties of NiO films prepared by sol–gel, Solar Energy, 83 (2009) 2103-2108.

[43] D.H. Jang, Y.J. Shin, S.M. Oh, Dissolution of Spinel Oxides and Capacity Losses in 4 V Li / $Li_xMn_2O_4$ Cells, Journal of The Electrochemical Society, 143 (1996) 2204-2211.

[44] T. Yoon, S. Park, J. Mun, J.H. Ryu, W. Choi, Y.-S. Kang, J.-H. Park, S.M. Oh, Failure mechanisms of $LiNi_{0.5}Mn_{1.5}O_4$ electrode at elevated temperature, Journal of Power Sources, 215 (2012) 312-316.

[45] S. Chae, J. Soon, H. Jeong, T.j. Lee, J.H. Ryu, S.M. Oh, Passivating film artificially built on $LiNi_{0.5}Mn_{1.5}O_4$ by molecular layer deposition of (pentafluorophenylpropyl)trimethoxysilane, Journal of Power Sources, 392 (2018) 159-167.

[46] D. Aurbach, E. Zinigrad, Y. Cohen, H. Teller, A short review of failure mechanisms of lithium metal and lithiated graphite anodes in liquid electrolyte solutions, Solid State Ionics, 148 (2002) 405-416.

[47] S. Flandrois, B. Simon, Carbon materials for lithium-ion rechargeable batteries, Carbon, 37 (1999) 165-180.

[48] S. Jurng, S. Park, T. Yoon, H.-s. Kim, H. Jeong, J.H. Ryu, J.J. Kim, S.M. Oh, Low-Temperature Performance Improvement of Graphite Electrode by Allyl Sulfide Additive and Its Film-Forming Mechanism, Journal of The Electrochemical Society, 163 (2016) A1798-A1804.

[49] J.H. Ryu, J.W. Kim, Y.-E. Sung, S.M. Oh, Failure Modes of Silicon Powder Negative Electrode in Lithium Secondary Batteries, Electrochemical and Solid-State Letters, 7 (2004) A306-A309.

[50] J.G. Lee, J. Kim, J.B. Lee, H. Park, H.-S. Kim, J.H. Ryu, D.S. Jung, E.K. Kim, S.M. Oh, Mechanical Damage of Surface Films and Failure of Nano-Sized Silicon Electrodes in Lithium Ion Batteries, Journal of The Electrochemical Society, 164 (2017) A6103-A6109.

[51] X. Zhang, T.M. Devine, Identity of Passive Film Formed on Aluminum in Li-Ion Battery Electrolytes with $LiPF_6$, Journal of The Electrochemical Society, 153 (2006) B344.

[52] S.F. Lux, I.T. Lucas, E. Pollak, S. Passerini, M. Winter, R. Kostecki, The mechanism of HF formation in $LiPF_6$ based organic carbonate electrolytes, Electrochemistry Communications, 14 (2012) 47-50.

[53] J.L. Tebbe, A.M. Holder, C.B. Musgrave, Mechanisms of $LiCoO_2$ Cathode Degradation by Reaction with HF and Protection by Thin Oxide Coatings, ACS Applied Materials and Interfaces, 7 (2015) 24265-24278.

[54] H.C. Genuino, N.N. Opembe, E.C. Njagi, S. McClain, S.L. Suib, A review of hydrofluoric acid and its use in the car wash industry, Journal of Industrial and Engineering Chemistry, 18 (2012) 1529-1539.

[55] A. Hammami, N. Raymond, M. Armand, Runaway risk of forming toxic compounds, Nature, 424 (2003) 635.

[56] J. Kim, H.-s. Kim, J.G. Lee, H. Jeong, J.H. Ryu, S.M. Oh, Communication—A Phosphorus Pentafluoride Scavenger to Suppress Solid Electrolyte Interphase Damage at Moderately Elevated

Temperature, Journal of The Electrochemical Society, 164 (2017) A3699-A3701.

[57] S. Jurng, H.-s. Kim, J.G. Lee, J.H. Ryu, S.M. Oh, Low-Temperature Characteristics and Film-Forming Mechanism of Elemental Sulfur Additive on Graphite Negative Electrode, Journal of The Electrochemical Society, 163 (2016) A223-A228.

[58] M. Xu, L. Zhou, L. Hao, L. Xing, W. Li, B.L. Lucht, Investigation and application of lithium difluoro(oxalate)borate (LiDFOB) as additive to improve the thermal stability of electrolyte for lithium-ion batteries, Journal of Power Sources, 196 (2011) 6794-6801.

[59] S. Park, J. Heon Ryu, S.M. Oh, Passivating Ability of Surface Film Derived from Vinylene Carbonate on Tin Negative Electrode, Journal of The Electrochemical Society, 158 (2011) A498-A503.

[60] L. Xiao, X. Ai, Y. Cao, H. Yang, Electrochemical behavior of biphenyl as polymerizable additive for overcharge protection of lithium ion batteries, Electrochimica Acta, 49 (2004) 4189-4196.

[61] K. Matsumoto, R. Kuzuo, K. Takeya, A. Yamanaka, Effects of CO2 in air on Li deintercalation from $LiNi_{1-x-y}Co_xAl_yO_2$, Journal of Power Sources, 81-82 (1999) 558-561.

[62] D. Aurbach, K. Gamolsky, B. Markovsky, G. Salitra, Y. Gofer, U. Heider, R. Oesten, M. Schmidt, The Study of Surface Phenomena Related to Electrochemical Lithium Intercalation into Li_xMO_y Host Materials (M = Ni, Mn), Journal of The Electrochemical Society, 147 (2000) 1322-1331.

[63] D. Takamatsu, Y. Orikasa, S. Mori, T. Nakatsutsumi, K. Yamamoto, Y. Koyama, T. Minato, T. Hirano, H. Tanida, H. Arai, Y. Uchimoto, Z. Ogumi, Effect of an Electrolyte Additive of Vinylene Carbonate on the Electronic Structure at the Surface of a Lithium Cobalt Oxide Electrode under Battery Operating Conditions, The Journal of Physical Chemistry C, 119 (2015) 9791−9797.

[64] M. Moshkovich, M. Cojocaru, H.E. Gottlieb, D. Aurbach, The study of the anodic stability of alkyl carbonate solutions by in situ FTIR spectroscopy, EQCM, NMR and MS, Journal of Electroanalytical Chemistry, 497 (2001) 84−96.

[65] K. Kanamura, S. Toriyama, S. Shiraishi, M. Ohashi, Z.−i. Takehara, Studies on electrochemical oxidation of non−aqueous electrolyte on the $LiCoO_2$ thin film electrode, Journal of Electroanalytical Chemistry, 419 (1996) 77−84.

[66] R. Crowe, J.P.S. Badyal, Surface modification of poly(vinylidene difluoride)(PVDF) by LiOH, Journal of the Chemical Society, Chemical Communications, (1991) 958−959.

[67] T. Yoon, D. Kim, K.H. Park, H. Park, S. Jurng, J. Jang, J.H. Ryu, J.J. Kim, S.M. Oh, Compositional Change of Surface Film Deposited on $LiNi_{0.5}Mn_{1.5}O_4$ Positive Electrode, Journal of The Electrochemical Society, 161 (2014) A519−A523.

[68] L. Yang, B. Ravdel, B.L. Lucht, Electrolyte Reactions with the Surface of High Voltage $LiNi_{0.5}Mn_{1.5}O_4$ Cathodes for Lithium−Ion

Batteries, Electrochemical and Solid-State Letters, 13 (2010) A95-A97.

[69] N.N. Sinha, A.J. Smith, J.C. Burns, G. Jain, K.W. Eberman, E. Scott, J.P. Gardner, J.R. Dahn, The Use of Elevated Temperature Storage Experiments to Learn about Parasitic Reactions in Wound $LiCoO_2$/Graphite Cells, Journal of The Electrochemical Society, 158 (2011) A1194-A1201.

[70] Y.-M. Song, C.-K. Kim, K.-E. Kim, S.Y. Hong, N.-S. Choi, Exploiting chemically and electrochemically reactive phosphite derivatives for high-voltage spinel $LiNi_{0.5}Mn_{1.5}O_4$ cathodes, Journal of Power Sources, 302 (2016) 22-30.

[71] E. Markevich, R. Sharabi, H. Gottlieb, V. Borgel, K. Fridman, G. Salitra, D. Aurbach, G. Semrau, M.A. Schmidt, N. Schall, C. Bruenig, Reasons for capacity fading of $LiCoPO_4$ cathodes in $LiPF_6$ containing electrolyte solutions, Electrochemistry Communications, 15 (2012) 22-25.

[72] B.V.R. Chowdari, K.F. Mok, J.M. Xie, R. Gopalakrishnan, Electrical and structural studies of lithium fluorophosphate glasses, Solid State Ionics, 76 (1995) 189-198.

[73] M. Murakami, H. Yamashige, H. Arai, Y. Uchimoto, Z. Ogumi, Direct Evidence of LiF Formation at Electrode/Electrolyte Interface by 7Li and 19F Double-Resonance Solid-State NMR Spectroscopy, Electrochemical and Solid-State Letters, 14 (2011) A134-A137.

[74] H. Park, T. Yoon, Y. Kim, J.G. Lee, J. Kim, H.-s. Kim, J.H. Ryu, J.J. Kim, S.M. Oh, Thermal Behavior of Solid Electrolyte Interphase Films Deposited on Graphite Electrodes with Different States-of-Charge, Journal of The Electrochemical Society, 162 (2015) A892-A896.

국문초록

$LiCoO_2$ 전극 표면필름의 고온 퇴화와 이의 전지특성 영향 및 그 완화방안

정 혜정

서울대학교 대학원

화학생물공학부

리튬이온 이차전지는 근래에 소형전자기기, 전동공구, 전기자동차, 대용량저장장치 등에 활발히 사용되고 있다. 그것은 오용이나 남용으로 인해 권장작동온도 이상의 고온(60~100°C)에 노출될 수 있다. 한편, 고온에서 전지용량은 퇴화한다. 따라서 그 퇴화 원인을 밝히는 일은 중요하다.

전지는 작동 전압 조건에서 필연적으로 전해액이 산화/환원하여, 전극 위에 표면필름을 만든다. 이 표면필름은 전기적 부동태 능력을 가져, 추가 전해액 산화를 막는 긍정적 역할을 한다. 음극에서는, 표면필름이 파괴되어 부동태 능력을 잃게 되면, 파괴된 표면 위에서 전해액이 산화하고 새로운 필름이 재생성된다. 이로써 전지의 용량이 줄어들고 그 수명을 단축시키며, 열폭주 기작의 발단이 되기도 한다. 한편, 음극에 비하여 양극(대표적으로 $LiCoO_2$)의 표면필름에 대한 그 연구는 부족하다.

위의 논의를 바탕으로, 양극 표면필름의 고온 퇴화와 이로 인한 전지특성 영향을 밝히고 그 완화방안을 제안하고자 하였다. 첫째, 양극 표면필름이 고온에서 퇴화하는지, 그 원인은 무엇인지, 그리고 필름 퇴화가 전지특성에 어떤 영향을 미치는지 밝히고자 하였다. 둘째, 고온에서 충전심도가 높은 경우의 표면필름 거동과 그것의 전지특성 영향을 밝히고자 하였다. 셋째, 퇴화 원인인 불화수소를 제거하기 위해 산화구리를 전극에 추가하여, 표면필름 퇴화를 억제함으로써 전지의 고온열화 완화를 모색하였다.

고온 노출을 시뮬레이션하기 위하여, $Li/LiCoO_2$ 전지를 제작하여 상온에서 수 회 충방전하여 $LiCoO_2$ 전극 표면필름을 만든 뒤, 고온 보관하였다. 고온 필름퇴화를 밝히고자, 전지를 완전 방전하여 보관하였고, 충전심도에 따른 영향을 밝히고자, 일정심도 충전 후 보관하였다. 고온보관 후, 전지를 상온에서 충방전하여 고온에서 겪은 전지의 변화를 확인하였다. 산화구리가 추가된 $LiCoO_2$ 전극으로 동일한

보관실험을 하였다. 사후분석 실험으로, 표면분석장비인 XPS, TEM, SEM 등을 활용하였다.

그 결과, 첫째, 70 °C 고온에서 표면필름은 퇴화하며, $LiPF_6$ 고온분해 후 생성된 불화수소의 공격에서 기인함을 밝혔다. 보관 후 상온에서 충방전 시, 표면필름이 퇴화된 $LiCoO_2$ 표면 위에서 전해액이 산화되어, $Li/LiCoO_2$ 전지의 충전용량이 증가하고 쿨롱효율이 퇴화함을 밝혔다. 둘째, 충전심도를 높게 고온보관하는 경우, 표면필름 퇴화 후 전해액산화로 인하여 표면필름이 재생성됨을 밝혔다. 표면필름이 재생성되어, 보관 후 상온에서 추가 전해액산화는 일어나지 않지만, 고온저장 중 용량이 손실되는 퇴화를 겪음을 밝혔다. 이는 앞의, 방전상태로 보관하여 표면필름이 완전 퇴화한 경우와 다른 퇴화 거동이다. 마지막으로, 불화수소 흡착제를 전극에 첨가하여 고온 불화수소 농도를 낮추면, 표면필름 퇴화가 지연되어, 고온보관 후 상온 충전용량 증가완화 및 고온보관 중 용량손실 완화를 이끌어낼 수 있음을 확인하였다.

주요어 : $LiCoO_2$ 전극; 고온퇴화; 표면필름; 표면필름 퇴화; 표면필름 재생성; 불화수소;

학번 : 2014-30294